R. & M. No. 3725

MINISTRY OF DEFENCE (PROCUREMENT EXECUTIVE)

AERONAUTICAL RESEARCH COUNCIL

REPORTS AND MEMORANDA

Calculation of the Induced Velocity Field on and off the Wing Plane for a Swept Wing with Given Load Distribution

By C. C. L. SELLS

Aerodynamics Dept., R.A.E. Farnborough

LONDON: HER MAJESTY'S STATIONERY OFFICE

1973

PRICE £1·55 NET

Calculation of the Induced Velocity Field on and off the Wing Plane for a Swept Wing with Given Load Distribution

By C. C. L. SELLS
Aerodynamics Dept., R.A.E., Farnborough

Reports and Memoranda No. 3725*
August, 1970

Summary

Computer programs have been written to evaluate the integrals of lifting-surface theory for the velocity field of a thin wing with given load distribution. Different programs are used for the downwash at points on the wing, and for any or all three velocity components off the wing. The heart of the programs is an analytic evaluation of the spanwise integral over a short line following the local sweep; by combining together a number of such integrals, the complete integral over the wing is built up. Both programs are tested by comparison with other results: exact linear theory for a two-dimensional flat plate, a result of Garner for a rectangular wing, theory for an infinite swept wing with isobars kinked at the centre line, and comparison for a tapered wing with a pioneer program written by Freestone. The downwash program cannot compute the downwash at the apex of a swept wing with rounded isobars, nor exactly at a wing tip.

* Replaces R.A.E. Technical Reports 69231 and 70146 (A.R.C. 32 144 and 32 549)

LIST OF CONTENTS

1. Introduction

The fundamental equation of linearized theory for a lifting wing in a uniform flow (lifting surface theory) gives the downwash at any point in the plane of the wing as an integral of the wing loading over the planform. This result gives the solution to the wing warp design problem. For the off-design problem it forms the basis of the collocation methods of Multhopp[1] type, and of the approximations[2] leading to the standard R.A.E. method.[3] However, Garner[4] has questioned the accuracy of the collocation methods, and a check on both these and the R.A.E. method would be useful. A computer program to evaluate the downwash integral directly and accurately, given the wing loading and planform, would provide such a check.

Freestone[5] has written a pioneer program, which imposes a rectangular computing grid on the physical planform, suitably refined near the 'control point' where the downwash is required and where the integrand is singular. This gives good results for the centre section of a rectangular wing,[5] but we expect less accuracy for swept or curved planforms, because then the rectangular grid no longer follows the leading and/or trailing edges. This difficulty is aggravated by the leading edge singularity of linear theory in the loading.

For these reasons, an improved program was required. Moreover, sometimes—e.g. to extend the benefit of the sweep effect on the critical Mach number into the centre—we are interested in load distributions with kinked isobars at the centre section of swept wings, and since this means the downwash has a logarithmic singularity at the kink in the plane ($z = 0$) of the doublet distribution representing the lifting surface, it was felt worthwhile to write a version of the program to calculate the more general downwash integral for points off this plane, that is $z \neq 0$, in order to improve centre section design methods. This version may also be applied later to the wing-fuselage interaction problem.

The program for $z = 0$ is actually a modification of the program for $z \neq 0$, and both programs work in basically the same way. We transform to a new chordwise variable ϕ (just as in the collocation methods) so that the leading and trailing edges form two co-ordinate lines, and the (normally inverse square root) singularity in the loading at the leading edge becomes easy to handle. This avoids the difficulties associated with Freestone's method, mentioned above. The wing is partitioned spanwise into a number of narrow strips running from the leading edge to the trailing edge; any cranks must be included as partition lines, but otherwise the method of partition is at our disposal. On any strip a given value of the new chordwise variable ϕ corresponds to a short line across the strip; on this short line the loading is approximated by a quadratic polynomial in the spanwise co-ordinate. Then the spanwise integration over this short line is done analytically (the case $z = 0$ requires special treatment) and by repeating this process for several suitable values of ϕ and applying the trapezoidal rule chordwise the double integral over the complete strip is built up. Finally, the contributions from all the strips are added up to give the integral over the whole wing.

For z small but not zero, the chordwise variation of the spanwise integral across the strip containing the control point is quite rapid near this point but always bounded, and by taking a sufficient number of values of ϕ near the control point, we can calculate the whole contribution from this strip as accurately as we please. When $z = 0$, it is necessary (in the present version of the program) to arrange that the control point shall lie strictly between two partition lines forming the limits of the spanwise integration, which is otherwise divergent all along the chord. (Even then, two chordwise singularities appear at the control point, but these can be handled without trouble.)

This means that the downwash cannot be evaluated on crank stations, and a special routine is needed to deal with the centre line of a swept wing.

This problem can be tackled in another way: instead of putting $z = 0$, we can put $y = 0$ first, and then we find that when the quadratic polynomial expression for the load distribution is introduced to allow analytic spanwise integration across a small strip adjoining the centre line, the contributions of the first two terms (for $y = 0$, $z \neq 0$) to the following chordwise integration show logarithmic infinities as $z \to 0$. One of these is the one that arises when a distribution of kinked isobars is imposed. We show that when the isobars are rounded, the two singularities cancel; two other terms containing products of z with divergent integrals can be evaluated in the limit $z \to 0$ and the remaining terms can be dealt with as before.

The method is not completely satisfactory, as there is a mathematical defect: at the apex of a swept wing, because of the proximity of port and starboard leading-edge loading singularities the three-term expression for the loading breaks down. Since this is only a contribution to an integral, one hopes that by choosing a sufficiently fine mesh near the apex the resulting inaccuracy can be kept small for control points a few mesh points down the chord, but the downwash can never be evaluated at the apex itself.

For some applications, it is convenient to be able to compute streamwash and sidewash also (for $z \neq 0$), and the relevant formulae are given in an Appendix. Any or all velocity components may be calculated in a run.

The program is written for incompressible flow. By the Prandtl–Glauert rule, it may be applied to subsonic flows by working with the analogous wing.

2. The Downwash Integral in Subsonic Lifting-Surface Theory

The downwash integral in linear theory for $z \neq 0$ is not so familiar as that for $z = 0$, so we derive it briefly here.

In the usual Cartesian axes centred on the wing apex with $0x$ downstream, $0y$ to starboard and $0z$ upwards, let the perturbation potential be φ, giving a perturbation velocity field $\mathbf{u} = \nabla\varphi$ superposed on the uniform free-stream $(U, 0, 0)$. Let the density and pressure be ρ, p; use subscripts u and l to denote values on upper and lower surfaces of the wing: then by Bernoulli's equation with squares neglected, the loading l on the wing is

$$l(x, y) = \frac{p_l - p_u}{\frac{1}{2}\rho U^2} = \frac{2}{U}\frac{\partial}{\partial x}(\varphi_u - \varphi_l). \tag{1}$$

Define

$$\Phi = \varphi_u - \varphi_l, \tag{2}$$

so that (1) gives

$$\frac{\partial \Phi}{\partial x} = \tfrac{1}{2}U l(x, y). \tag{3}$$

The discontinuity Φ in the harmonic function φ on the wing, and wake, which in linearized theory are assumed to lie in the plane $z = 0$, can be represented by a doublet distribution in this plane with the doublet axes in the z direction:

$$\varphi(x, y, z) = -\frac{1}{4\pi}\iint_{z=0} \Phi(X, Y)\frac{\partial}{\partial z}\left(\frac{1}{r}\right) dX\, dY \tag{4}$$

where

$$r^2 = (X - x)^2 + (Y - y)^2 + z^2. \tag{5}$$

Integrating by parts with respect to X,

$$\begin{aligned}
\varphi(x, y, z) &= \frac{1}{4\pi}\iint_{z=0} \Phi(X, Y)\frac{z}{r^3} dX\, dY \\
&= \frac{z}{4\pi}\iint_{z=0} \frac{\Phi(X, Y)}{(Y - y)^2 + z^2}\frac{\partial}{\partial X}\left\{C(Y, z) + \frac{X - x}{r}\right\} dX\, dY \\
&= \frac{z}{4\pi}\int \left[\frac{\Phi(X, Y)}{(Y - y)^2 + z^2}\left\{C(Y, z) + \frac{X - x}{r}\right\}\right]_{X=-\infty}^{X=\infty} dY \\
&\quad - \frac{z}{4\pi}\iint_{z=0} \frac{\partial\Phi/\partial X}{(Y - y)^2 + z^2}\left\{C(Y, z) + \frac{X - x}{r}\right\} dX\, dY.
\end{aligned} \tag{6}$$

Now, far upstream ($X = -\infty$) there is no potential discontinuity so $\Phi = 0$, and the term in curly brackets vanishes far downstream ($X = \infty$) if $C(Y, z)$ is chosen equal to -1. Also in the integral of (6) $\Phi = 0$ everywhere upstream of the wing, and downstream of it the wake cannot support a pressure difference, so from (3) $\partial\Phi/\partial x = 0$ on the wake, and the double integral is taken over the wing alone:

$$\varphi(x, y, z) = \frac{z}{4\pi}\iint_{\text{wing}} \frac{\frac{1}{2}U l(X, Y)}{(Y - y)^2 + z^2}\left\{1 - \frac{X - x}{r}\right\} dX\, dY,$$

so the downwash $\alpha = -(1/U)(\partial\varphi/\partial z)$ is

$$\alpha(x, y, z) = -\frac{1}{8\pi}\frac{\partial}{\partial z}z\iint_{\text{wing}} \frac{l(X, Y)}{(Y - y)^2 + z^2}\left(1 - \frac{X - x}{r}\right) dX\, dY. \tag{7}$$

3. Transformation of the Integral

The task at hand is the evaluation of the double integral (7) for some points (x, y, z), where z may or may not be zero, when the planform S is given, along with a load distribution $l(X, Y)$ which will have singularities on the planform edges.[2] When $z = 0$, the integrand also has a line singularity $Y = y$ and a point singularity at the control point $(X, Y) = (x, y)$; when $z \neq 0$ these last are absent in the mathematical sense, but since z may be a fraction of a per cent of the local chord, the integrand will not be numerically well-behaved near this line $Y = y$ (we may call it the control line). The first part of the kernel of (7)

$$\partial/\partial z[z/\{(Y - y)^2 + z^2\}],$$

considered as a function of Y, has a minimum value $-1/z^2$ at $Y = y$, and two maxima values $+1/8z^2$ at $Y = y \pm z\sqrt{3}$, which is sufficient to demonstrate the point.

To overcome this obstacle for small z, we try to choose a spanwise neighbourhood of $Y = y$ small enough for a simple representation of the loading l to be accurate, and then we can perform the spanwise integration across this neighbourhood analytically, leaving only the chordwise integration to be done numerically. So we partition the wing spanwise by a number of straight lines $Y =$ constant, *see* Fig. 1; the loading can be specified as data along each partition line, and typically by using information on three consecutive partition lines for each chordwise position ($A'B'C'$, say, in Fig. 1) we can fit a parabolic interpolation function across the strip bounded by two of them and then integrate spanwise over the strip. Normally the way we group these partition lines by threes is at our disposal, and we try to arrange the grouping so that the control line lies strictly inside an integration strip (AC, say, in Fig. 1); then the first derivative of the interpolate is continuous at the control line (this corresponds to unkinked isobars) and we avoid introducing spurious logarithmic terms (we know this from experience, but it will also be clear later when the analysis is complete).

First, it is convenient to transform the chordwise variable X to a new one ϕ such that the leading and trailing edges become co-ordinate lines and the singularities in the loading at these edges become numerically tractable. The transformation is standard and the same as that used in the collocation or R.A.E. standard methods: if the leading edge is given by $x = x_L(y)$ and the chord by $c = c(y)$, the transformation is

$$X = x_L(Y) + \tfrac{1}{2}c(Y)(1 - \cos\phi). \tag{8}$$

Then the leading and trailing edges correspond to $\phi = 0$ and $\phi = \pi$ respectively. In Fig. 1, A', B', C' correspond to the same value of ϕ. The integral (7) is now written in the form

$$\alpha = -\frac{1}{8\pi}\sum_{\text{strips}}\frac{1}{2}\int_0^\pi d\phi\frac{\partial}{\partial z}z\int_{\text{strip}}dY\frac{L(\phi, Y)}{(Y - y)^2 + z^2}\left(1 - \frac{X - x}{r}\right) \tag{9}$$

where

$$L(\phi, Y) = l(X, Y)c(Y)\sin\phi.$$

Since $l(X, Y)$ usually behaves like $(X - x_L)^{-\frac{1}{2}}$ near the leading edge, while $\sin\phi$ behaves like $(X - x_L)^{\frac{1}{2}}$, the product L is usually well-behaved and finite there, and similarly at the trailing edge where L usually goes to zero quadratically in $(\pi - \phi)$.

In dealing with the spanwise integration across a typical strip, it saves trouble to change the origin to the point $Y = y$ and adjust the limits of integration accordingly, since then y does not appear explicitly in the integrand. We write

$$Y - y = \eta \tag{10}$$

and expand $L(\phi, Y)$ for constant ϕ as a three-term Taylor series in η:

$$L(\phi, Y) = g_0 + \eta g_1 + \eta^2 g_2. \tag{11}$$

This representation is to be valid in the strip $\eta_- \leqslant \eta \leqslant \eta_+$, say, even though the strip does not in general include the point $\eta = 0$. Figure 2 shows such a case. Thus the contributions from g_0, g_1, g_2 are not necessarily in decreasing order. This is the price we pay for the simplification (10). It is a small price, because (11) is always derived from a local expansion about some point η^*, say, which *is* in the strip.

In the same way we find an expression for the term $X - x$ in (9). Introducing the local section co-ordinate ξ by

$$X = x_L(Y) + c(Y)\xi \tag{12}$$

so that $\xi = \frac{1}{2}(1 - \cos\phi)$ and hence ξ is constant along the lines ϕ = constant, we see that the variation of $(X - x)$ is entirely due to the variation of $x_L(Y)$ and $c(Y)$ across the strip. Looking again at (9), we see that because of the presence of r given by (5), we must be content with a linear variation in Y or η of these two geometric parameters, or else the spanwise integral of (9) will become an elliptic integral and we shall not be able to evaluate it analytically. This should not greatly disturb us since swept-wing planforms of current interest do frequently have their leading and trailing edges made up of straight-line segments, but it does mean that we may need many small integration strips in our partitioning when curved planforms with rapid sweep changes are studied, and it also requires—reasonably enough—that cranks in the planform shall lie on partition lines, and we may not integrate at one step across a strip with a crank in its interior.

Fitting straight lines to $x_L(Y)$ and $c(Y)$ in the range $\eta_- \leqslant \eta \leqslant \eta_+$, if η^* is a reference point in this range then

$$\begin{aligned} x_L(Y) &= x_L(y + \eta^*) + (Y - y - \eta^*)x_L'(y + \eta^*) \\ &= x_L^* + \eta x_L'(y + \eta^*) \end{aligned} \tag{13}$$

where $x_L^* = x_L(y + \eta^*) - \eta^* x_L'(y + \eta^*)$; we remark that in general x_L^* is not equal to $x_L(y)$ because there may be cranks or leading edge curvature present. The physical significance of x_L^* is indicated in Fig. 3. $x_L'(y + \eta^*)$ is taken constant across the strip and we may write it just x_L'. Similarly, we have

$$c(Y) = c^* + \eta c' \tag{14}$$

where $c^* = c(y + \eta^*) - \eta^* c'(y + \eta^*)$, *see* Fig. 3; and so (12) gives

$$\begin{aligned} X - x &= (x_L^* + c^*\xi - x) + \eta(x_L' + c'\xi) \\ &= h + \eta a \end{aligned} \tag{15}$$

$a = x_L' + c'\xi$ is recognised as the local sweep at (X, Y). The physical significance of h, for a given ξ, is also indicated in Fig. 3. We can now write (9) in the form

$$\alpha = -\frac{1}{8\pi} \sum_{\text{strips}(\eta_-, \eta_+)} \frac{1}{2} \int_0^\pi d\phi[\alpha_1(\eta_+) - \alpha_1(\eta_-)] \tag{16}$$

$$\alpha_1 = \frac{\partial \hat{I}}{\partial z} = g_0 I_0 + g_1 I_1 + g_2 I_2 \tag{17}$$

$$\hat{I} = z \int d\eta \frac{g_0 + g_1\eta + g_2\eta^2}{\eta^2 + z^2} \left(1 - \frac{h + \eta a}{r}\right) = g_0 \hat{I}_0 + g_1 \hat{I}_1 + g_2 \hat{I}_2 \tag{18}$$

$$r^2 = (h + \eta a)^2 + \eta^2 + z^2. \tag{19}$$

making use of (5), (11) and (15).

It may be verified by direct differentiation that

$$\frac{\partial}{\partial \eta} \arctan \frac{zr}{\eta h - z^2 a} = -\frac{z}{r} \frac{h + \eta a}{z^2 + \eta^2}$$

and so

$$\begin{aligned} \hat{I}_0 &= \left\{ -\arctan \frac{z}{\eta} + \arctan \frac{zr}{\eta h - z^2 a} \right\} \\ I_0 &= \frac{\partial \hat{I}_0}{\partial z} = -\frac{\eta}{\eta^2 + z^2} + \frac{h\eta(r^2 + z^2) + az^2(r^2 - z^2)}{r(h^2 + b^2 z^2)(\eta^2 + z^2)}. \end{aligned} \tag{20}$$

Here we have written

$$b^2 = 1 + a^2. \tag{21}$$

Again, the g_1 integral of (18) can be written

$$\hat{I}_1 = z \ln (r + h + \eta a) - z(a/b) \ln f \tag{22}$$

with

$$f = r + \eta b + ha/b. \tag{23}$$

Differentiating (22) with respect to z, we have

$$I_1 = \ln (r + h + \eta a) + \frac{z^2}{r(r + h + \eta a)} - \frac{a}{b}\left(\ln f + \frac{z^2}{rf}\right). \tag{24}$$

Finally, we have after manipulation

$$\hat{I}_2 = z\left(\eta - \frac{a}{b^2} r - \frac{h}{b^3} \ln f\right) - z^2 \hat{I}_0.$$

Differentiating with respect to z,

$$I_2 = \eta - \frac{a}{b^2} r - \frac{h}{b^3} \ln f - z\left(\frac{a}{b^2}\frac{z}{r} + \frac{h}{b^3}\frac{z}{rf}\right) - 2z\hat{I}_0 - z^2 I_0. \tag{25}$$

4. Integration Outboard of Root on the Wing Plane ($z = 0$)

Let us consider the evaluation of (16) from the standpoint of the classical problem posed by (7) for the downwash on the plane $z = 0$ of linearized theory. In dealing with the spanwise singularity (7) Mangler has shown[1] how to define the finite part for the spanwise integral—which is otherwise divergent—by retaining $z \neq 0$ and carrying out the analysis before letting $z \to 0$. The analysis here is complicated by the change of coordinates and the extra terms we have brought in, but the general principle is the same: the vital spanwise integration across the control section is done first, then z is allowed to vanish.

By formally putting $z = 0$, we have

$$I_0(\phi, \eta, 0) = \frac{1}{\eta}\left(\frac{r_0}{h} - 1\right) = \frac{r_0 - h}{\eta h} \tag{26}$$

where

$$r_0^2 = (h + \eta a)^2 + \eta^2; \qquad f_0 = r_0 + \eta b + ha/b; \tag{27}$$

and

$$I_1(\phi, \eta, 0) = \ln (r_0 + h + \eta a) - \frac{a}{b} \ln f_0 \tag{28}$$

$$I_2(\phi, \eta, 0) = \eta - \frac{a}{b^2} r_0 - \frac{h}{b^3} \ln f_0. \tag{29}$$

Hence (17) gives

$$(\alpha_1)_{z=0} = g_0 I_0(\phi, \eta, 0) + g_1 \ln (r_0 + h + \eta a) - [g_1(a/b) + g_2(h/b^3)] \ln f_0 + g_2[\eta - (a/b^2) r_0] \tag{30}$$

The expression (30) is not suitable as it stands for the numerical chordwise integration which must be done next, because, as we shall see, there are two chordwise singularities. However, neither singularity is difficult to handle. The first one (with the coefficient g_0) gives an integral similar to the chordwise integral of linearized two-dimensional section theory, which is likewise defined as a Cauchy principal value, the second one is a (weaker)

logarithmic singularity ($\ln f_0$) which turns out easier to program than the first because it only appears when dealing with the control line integration strip, whereas the first one may appear (depending on the planform geometry) on all the integration strips.

The method used is standard, but it is well to set down the details for reference. We shall consider each singularity in turn.

We begin with the contribution from I_0 in (26) to (30); putting in the integration limits from (16), we have

$$\alpha_{10} = g_0\left[\frac{r_0 - h}{h\eta}\right]_{\eta_-}^{\eta_+}. \tag{31}$$

We note in passing that this becomes infinite also when one of the limits of integration η_+ or η_- is zero. Thus (31) cannot be used to find the downwash (for $z = 0$) on crank stations, which are natural integration boundaries in our method.

Even when $\eta_\pm$ is not zero, equation (31) certainly has an infinity on the control strip where $h = 0$. By equations (13) through (15), with $\eta^* = 0$, this occurs at the control point where ξ (and ϕ, by (12)) is given by $x_L(y) + c(y)\xi = x$. By (15) h varies linearly with ξ so the chordwise integral of α_{10} has a simple Cauchy principal value. The analogy with the result for two-dimensional sections (or infinite sheared wings) may be seen by inserting the limits $\eta_\pm = \pm\infty$, for which

$$\lim (r_0 - h)/\eta_\pm = \pm b.$$

The spanwise loading is constant, so $g_0 \equiv g_0(\xi)$, $g_1 = g_2 = 0$ and the two-dimensional result follows.

To deal with the chordwise integration of (31), for a general strip, consider

$$\beta = g_0(\phi)\left[\frac{r_0 - h}{\eta}\right]_{\eta_-}^{\eta_+} \tag{32}$$

g_0 is a function of ϕ as far as any particular integration strip is concerned. Noting that, when $h = 0$ (27) gives

$$r_0 = |\eta| b \tag{33}$$

we find

$$\lim_{h\to 0} \beta \equiv \beta_c = g_0(\phi_c) b_c (\operatorname{sgn}\eta_+ - \operatorname{sgn}\eta_-). \tag{34}$$

The suffix c refers to conditions at $h = 0$ (the control point, on the control strip). From (34) we see that when η_+ and η_- have the same sign, that is for any integration strip other than the control one, $\beta_c = 0$ and there is only a ratio of two zeros to consider in (31); for the control strip, $\eta_- < 0$, $\eta_+ > 0$ and $\beta_c = 2g_0(\phi_c)b_c$.

We now consider the function

$$\alpha_{10} - \beta_c/h = (\beta - \beta_c)/h. \tag{35}$$

This function has a limit as $h \to 0$, which can be found by L'Hospital's rule. Noting from (27) and (15)

$$r_0 \frac{dr_0}{dh} = (h + \eta a)\left(1 + \eta \frac{da/d\xi}{dh/d\xi}\right)$$
$$= \eta a(1 + \eta c'/c^*) \quad \text{at } h = 0$$

the limit works out as

$$\frac{d\beta}{dh} = \left[\frac{dg_0(\phi)/d\phi}{\frac{1}{2}c^* \sin\phi} b + g_0 \frac{ac'}{bc}\right]_{\phi=\phi_c} (\operatorname{sgn}\eta_+ - \operatorname{sgn}\eta_-) + \left\{ g_0 \left[\frac{(a/b)\operatorname{sgn}\eta - 1}{\eta}\right]_{\eta_-}^{\eta_+} \right\}_{\phi=\phi_c}. \tag{36}$$

Like β_c the first term in (36) only has to be computed at the control point, and is zero elsewhere, but the second term does not vanish for the other integration strips. We employ (36) quite generally, instead of (35), whenever h becomes very small ($|h| < 10^{-4}$ in the program).

The chordwise integration now proceeds, using (35) rather than (31). The use of (35) implies an extra integral to be added on, given by

$$\beta_c \int_0^\pi \frac{d\phi}{h}. \tag{37}$$

Away from the control strip, $\beta_c = 0$; on the control strip, by (12) and (15)

$$h = \tfrac{1}{2}c(\cos\phi_c - \cos\phi)$$

and the integral vanishes, for all ϕ_c. Thus (35) entails no extra contribution at all, on any integration strip.

We turn next to the logarithmic singularity in (30). This is *not* due to the term $g_1 \ln(r_0 + h + \eta a)$, but we remark that if $\eta_\pm = 0$, $r_0 = |h|$ and so this logarithm will be infinite for $h < 0$; thus this expression, as well as (31), is forbidden for evaluation of downwash on crank stations when $z = 0$.

The singularity actually comes in the term

$$-\left(g_1\frac{a}{b} + g_2\frac{h}{b^3}\right)\ln f_0. \tag{38}$$

From (27) and (33) f_0 vanishes when $h = 0$ and $\eta > 0$. It is well behaved for $\eta < 0$, so integration strips to starboard of the control line are trouble-free; to deal with the port side, we remark that

$$(r_0 + \eta b + ha/b)(r_0 - \eta b - ha/b) = h^2/b^2 \tag{39}$$

so the expression

$$-(g_1 a/b + g_2 h/b^3)(\operatorname{sgn}\eta)\ln[r_0 + (\operatorname{sgn}\eta)(\eta b + ha/b)] \tag{40}$$

is identical with (38) when $\eta > 0$, differs from it by a term independent of η (which we can ignore) when $\eta < 0$, and is well-behaved for both $\eta > 0$ and $\eta < 0$, so we can use (40) to port and starboard, where no singularities will arise.

The control strip, with $\eta_+ > 0$, $\eta_- < 0$, again forms an exception, as we cannot use (40) on both sides at once without first introducing the constant on the right side of (39). This leads to

$$\alpha_{11} = -(g_1 a/b + g_2 h/b^3)\{[(\operatorname{sgn}\eta)\ln\{r_0 + (\operatorname{sgn}\eta)(\eta b + ha/b)\}]_{\eta_-}^{\eta_+} + 2\ln b - 2\ln|h|\}. \tag{41}$$

The last two terms in (41) come in only on the control strip. In this case, we integrate chordwise the function

$$\alpha_{11} - \beta_1 \ln|h| \tag{42}$$

where

$$\beta_1 = (2g_1 a/b)_{\phi=\phi_c}. \tag{43}$$

(42) is finite everywhere on the control strip, in particular at the control point where $h = 0$, but it does have a logarithmic infinity in slope there, so the chordwise refinement technique used for $z \neq 0$ will still be needed for $z = 0$ to deal with this term alone, unlike the function (35) which is perfectly well behaved near $h = 0$.

This time, to balance the β_1 term, we must add to the chordwise integral of (42) the integral

$$\beta_1 \int_0^\pi \ln|h|\, d\phi = \beta_1[\pi \ln\{\tfrac{1}{2}c(y)\} + J] \tag{44}$$

where

$$J = \int_0^\pi \ln|\cos\phi_c - \cos\phi|\, d\phi. \tag{45}$$

We find, as for (37), that $dJ/d\phi_c = 0$, so $J = \text{constant} = (J)_{\phi_c=\pi/2} = -\pi\ln 2$, and (44) becomes

$$\beta_1 \pi \ln\{\tfrac{1}{4}c(y)\}. \tag{46}$$

This completes the discussion of the chordwise singularities.

Collecting together these results, we find for (16) when $y \neq 0$

$$\alpha(x, y, 0) = -\frac{1}{8\pi}\left\{\left(g_1\frac{a}{b}\right)_{\phi_c} \pi \ln\{\tfrac{1}{4}c(y)\} + \sum_{\text{strips}} \frac{1}{2}\int_0^\pi d\phi([\alpha_0]_{\eta_-}^{\eta_+} + \alpha_2)\right\} \tag{47}$$

where

$$\alpha_0 = \left[g_0\frac{r_0 - h}{\eta} - (\operatorname{sgn}\eta)(g_0 b)_{\phi=\phi_c}\right]\frac{1}{h} + g_1 \ln(r_0 + h + \eta a) - \left(g_1\frac{a}{b} + g_2\frac{h}{b^3}\right)$$
$$\times (\operatorname{sgn}\eta)\ln\left\{r_0 + (\operatorname{sgn}\eta)\left(\eta b + \frac{ha}{b}\right)\right\} + g_2(\eta - r_0 a/b^2) \tag{48}$$

and

$$\alpha_2 = -2\delta\left[\left(g_1\frac{a}{b} + g_2\frac{h}{b^3}\right)(\ln b - \ln|h|) + \left(g_1\frac{a}{b}\right)_{\phi_c} \ln|h|\right]. \tag{49}$$

Here $\delta = 1$ for the control strip, and $\delta = 0$ elsewhere.

When $h \doteqdot 0$, by (36) the first term in α_0 must be replaced by

$$\left[\operatorname{sgn}\eta\left(\frac{dg_0/d\phi}{\frac{1}{2}c\sin\phi}b + g_0\frac{ac'}{bc}\right) + \frac{g_0}{\eta}\left(\frac{a}{b}\operatorname{sgn}\eta - 1\right)\right]_{\phi=\phi_c}. \tag{50}$$

5. Rounded Isobars at Wing Root, $y = z = 0$

The expressions derived in Section 4 are satisfactory when the control point (x, y) does not lie on the centre line (or another crank station), since a layout as in Fig. 1 can be chosen with $\eta_- < 0, \eta_+ > 0$. But when the control point is on the centre line, $y = 0$, we must choose the first integration strip with $\eta_- = 0, \eta_+ > 0$, and then (26) and (28) break down, although (29) is still all right.

To overcome this difficulty, we must manipulate (20) and (24) into different forms using the regularity of the loading at the centre line to remove the infinities which occur. This is explained next.

When the control point lies in the centre section $y = 0$, (16) can be written over only half the wing, by symmetry:

$$\alpha(x, 0, z) = -\frac{1}{8\pi}\left\{\int_0^\pi d\phi[\alpha_1(\eta_+) - \alpha_1(0)] + \sum_{\substack{\text{starboard strips} \\ \eta_- > 0}}^{(\eta_-, \eta_+)} \int_0^\pi d\phi[\alpha_1(\eta_+) - \alpha_1(\eta_-)]\right\}. \tag{51}$$

When $z = 0$ the terms in the outboard summation can be dealt with by the method of Section 4, but not the $\alpha_1(0)$ sub-term in the first term; it is this term which concerns us here. It is computationally convenient (we shall see that we do not have to calculate the local values $g_1(\phi)$, only g_0 and g_2, on the centre line) to treat $\alpha_1(\eta_+)$ as well as $\alpha_1(0)$, and so we hold both η and z in the formulae (20), (24) for the moment. For notational simplicity we also drop the suffix $+$ on η_+, as we shall not mention the outboard strips again in this section. It is also convenient to work with the local section coordinate ξ.

With the reference line $\eta^* = 0$ at the centre line $Y = 0$, we have

$$g_1 = \sin\phi \,.\, \partial[l(\xi, \eta)c(\eta)]/\partial\eta \tag{52}$$

where the derivative is evaluated at constant ϕ or ξ. Using (3), we write the potential difference $\Phi = \frac{1}{2}U\Delta$ where the loading $l = \partial\Delta/\partial X$. ($U$ is the free stream velocity.) With $X = x_L(\eta) + \xi c(\eta)$, $Y = \eta$, we have

$$\frac{\partial\Delta}{\partial\xi} = c(\eta)\frac{\partial\Delta}{\partial x} = c(\eta)l(\xi, \eta) \tag{53}$$

and

$$\frac{\partial\Delta}{\partial\eta} = (x_L' + \xi c')\frac{\partial\Delta}{\partial x} + \frac{\partial\Delta}{\partial y}.$$

Here $x'_L + c'\xi = a(\xi) =$ local sweep, *see* equation (15). Also, everywhere on the centre section except at leading edge and trailing edge, $\partial\Delta/\partial y = 0$ by the unswept-isobars condition. Hence, on the centre line, for $0 < \xi < 1$

$$\frac{\partial \Delta}{\partial \eta} = a(\xi) l(\xi, 0). \tag{54}$$

Using (52) and (53), we have

$$\int_0^\pi g_1(\phi) I_1 \, d\phi = 2 \int_0^1 \frac{\partial^2 \Delta}{\partial \xi \, \partial \eta} I_1 \, d\xi$$

$$= 2 \lim_{\rho \to 1} \int_0^\rho \frac{\partial^2 \Delta}{\partial \xi \, \partial \eta} I_1 \, d\xi$$

(since integrand is bounded near the trailing edge, so that the integral from ρ to 1 tends to 0 as $\rho \to 1$)

$$= 2 \lim_{\rho \to 1} \left\{ \left[\frac{\partial \Delta}{\partial \eta} I_1 \right]_0^\rho - \int_0^\rho \frac{\partial \Delta}{\partial \eta} \frac{\partial I_1}{\partial \xi} \, d\xi \right\}.$$

Now $\Delta \equiv 0$ at $\xi = 0$ (the leading edge) for all η, and so $\partial\Delta/\partial\eta = 0$ at $\xi = 0$. Also for $0 < \rho < 1$ $\partial\Delta/\partial\eta$ is given by (54) and so tends to 0 as $\rho \to 1$ by the Kutta condition. Thus the first term vanishes at both ends of the range. Using (54) we can rewrite the second term

$$-2 \lim_{\rho \to 1} \int_0^\rho a(\xi) l(\xi, 0) \frac{\partial I_1}{\partial \xi} \, d\xi.$$

The integrand is bounded near the trailing edge, so we can put $\rho = 1$. We now change the variable of integration back to ϕ, but we note that I_1 depends on ξ only through h, which is equal to $x_L^* + c^*\xi - x$ by (15) so that

$$\frac{\partial}{\partial \xi} = c^* \frac{\partial}{\partial h} = c \frac{\partial}{\partial h}$$

since $c^* = c$, the centre line being its own reference line. Thus finally

$$\int_0^\pi g_1(\phi) I_1 \, d\phi = -\int_0^\pi a(\xi) l(\xi, 0) c(0) \frac{\partial I_1}{\partial h} \sin \phi \, d\phi = -\int_0^\pi g_0(\phi) a(\phi) \frac{\partial I_1}{\partial h} \, d\phi. \tag{55}$$

With the help of (55) the first term inside the curly brackets of (51) is now written, in the notation of (17),

$$\int_0^\pi [g_0 I_0 + g_1 I_1 + g_2 I_2]_0^\eta \, d\phi = \int_0^\pi \left[g_0(\phi) \left(I_0 - a \frac{\partial I_1}{\partial h} \right) + g_2 I_2 \right]_0^\eta d\phi. \tag{56}$$

From (24)

$$\frac{\partial I_1}{\partial h} = \left(\frac{1}{r} - \frac{z^2}{r^3} \right) \left(1 + \eta \frac{c'}{c} \right) - \frac{a/b}{h^2 + b^2 z^2} \left[\frac{z^2 ab}{r} + h \left(1 - \frac{\eta b}{r} \right) \right]$$

$$- \frac{c'}{c} \left[\frac{\ln f}{b^3} + \frac{a}{bf} \left\{ \frac{(h + \eta a)\eta}{r} + \frac{a\eta}{b} + \frac{h}{b^3} \right\} \right] - \frac{\partial}{\partial h} \left(\frac{a}{b} \frac{z^2}{rf} \right). \tag{57}$$

The c' terms arise because a and b are not constants for a tapered wing, but vary with h; from (15)

$$\frac{\partial a}{\partial h} = \frac{\partial a}{\partial \xi} \frac{\partial \xi}{\partial h} = \frac{c'}{c}.$$

$$\frac{\partial}{\partial h} \frac{a}{b} = \frac{\partial a}{\partial h} \frac{d}{da} \frac{a}{(a^2 + 1)^{\frac{1}{2}}} = \frac{c'}{b^3 c}.$$

For $\eta \neq 0$, we let $z \to 0$ and combine (20) and (57) in (56) to give:

$$\left(I_0 - a\frac{\partial I_1}{\partial h}\right)(\phi, \eta, 0) = \frac{r_0 - h}{\eta h} - \frac{a}{r_0} + \frac{a^2}{bh}\left(1 - \frac{\eta b}{r_0}\right) + \frac{ac'}{c}\left[-\frac{\eta}{r_0} + \frac{\ln f_0}{b^3} + \frac{a}{bf_0}\left\{\frac{(h + \eta a)\eta}{r_0} + \frac{a\eta}{b} + \frac{h}{b^3}\right\}\right]. \tag{58}$$

For $\eta = 0$, retain $z \neq 0$ at first. Write

$$r_1 = [r]_{\eta=0} = (h^2 + z^2)^{\frac{1}{2}}$$
$$f_1 = [f]_{\eta=0} = r_1 + ha/b.$$

Then (20) gives

$$I_0(\phi, 0, z) = \frac{ah^2}{r_1(h^2 + b^2z^2)} = \frac{a}{r_1} - \frac{ab^2z^2}{r_1(h^2 + b^2z^2)}. \tag{59}$$

It is the first term on the right side of (59) that causes the infinity in the downwash on a thin wing with kinked isobars, since the integral

$$\int_0^{\pi} g_0(\phi)\frac{a}{r_1}\,d\phi = 2\int_{h_{L.E.}}^{h_{T.E}} l\frac{a}{r_1}\,dh$$

shows a logarithmic infinity for $z \to 0$. However, when the isobars are rounded the first term in $\partial I_1/\partial h$ given by (57) produces a term $1/r_1$ which cancels it out when the combination $I_0 - a\partial I_1/\partial h$ is taken in (56). In fact, at $\eta = 0$

$$\left(I_0 - a\frac{\partial I_1}{\partial h}\right)(\phi, 0, z) = -\frac{az^2}{r_1(h^2 + b^2z^2)} + \frac{az^2}{r_1^3} + \frac{a^2h}{b(h^2 + b^2z^2)} + \frac{c'}{c}\frac{a}{b^3}\left(\ln f_1 + \frac{ha}{bf_1}\right) + a\frac{\partial}{\partial h}\left(\frac{a}{b}\frac{z^2}{r_1 f_1}\right). \tag{60}$$

Now insert into (56) and consider the first two terms. We integrate over a small region containing the control point $\phi = \phi_c$, say, corresponding to $X = x, h = 0$; outside this region the integrand is well-behaved and tends to 0 as $z \to 0$. Putting

$$\phi = \phi_c + \frac{2\psi}{c \sin \phi_c},$$

and letting the small region correspond to $-\varepsilon \leqslant \psi \leqslant \varepsilon$, the first two terms in (60) contribute

$$\begin{aligned}
&\int g_0(\phi)\left[\frac{az^2}{r_1^3} - \frac{az^2}{r_1(h^2 + b^2z^2)}\right] d\phi \\
&= \int_{-\varepsilon}^{\varepsilon} [g_0(\phi_c)a(\phi_c) + 0(\psi)]\frac{2}{c \sin \phi_c}\left[\frac{z^2}{(\psi^2 + z^2)^{\frac{1}{2}}} - \frac{z^2}{(\psi^2 + z^2)^{\frac{1}{2}}(\psi^2 + b^2z^2)}\right] d\psi \\
&= \frac{2g_0(\phi_c)a(\phi_c)}{c \sin \phi_c}\left[\frac{\psi}{(\psi^2 + z^2)^{\frac{1}{2}}} - \frac{1}{2ab}\ln\frac{bz(\psi^2 + z^2)^{\frac{1}{2}} + a\psi z}{bz(\psi^2 + z^2)^{\frac{1}{2}} - a\psi z}\right]_{-\varepsilon}^{\varepsilon} + 0(z) \to \frac{4g_0(\phi_c)}{c \sin \phi_c}\left(a - \frac{1}{2b}\ln\frac{b + a}{b - a}\right)_c \\
&= 4l(x, 0)\left\{a_c - \frac{1}{b_c}\ln(b_c + a_c)\right\} \quad \text{as } z \to 0
\end{aligned} \tag{61}$$

making use of (21) and the definition of g_0 when the centre line is its own reference line. Thus, in spite of the presence of z^2 in the numerators, the first two terms of (60) make a finite contribution to the integral (56).

As $z \to 0$, the third term in (60) tends to the value (a^2/bh). This matches with a similar term in the expression (58), and so when taking the difference of the two limits η and 0 in (56) these two terms cancel.

The last term in (60) has no effect since the parallel analysis to (61) leads to

$$\frac{2g_0(\phi_c)a_c}{c \sin \phi_c}\frac{a}{b}\left[\frac{z^2}{r_1 f_1}\right]_{-\varepsilon}^{\varepsilon} \to 0 \qquad \text{as } z \to 0.$$

Collecting the results (29), (58), (60) and (61), and slightly simplifying the square brackets in (58), we have for the expression (56)

$$\int_0^\pi \left[g_0(\phi)\left(I_0 - a\frac{\partial I_1}{\partial h}\right) + g_2 I_2 \right]_0^\eta d\phi = -4\frac{g_0(\phi_c)}{c\sin\phi_c}\left\{ a_c - \frac{1}{b_c}\ln(b_c + a_c)\right\} + \int_0^\pi d\phi \left\{ g_0\left[\frac{1}{h}\left\{ \frac{r_0 - h}{\eta} - \frac{a^2\eta}{r_0}\right\} - \frac{a}{r_0}\right.\right.$$
$$\left. + \frac{ac'}{c}\left\{ \frac{\ln f_0}{b^3} + \frac{1}{f_0}\left(\frac{ha}{b^4} - \frac{\eta}{b^2} - \frac{\eta^2}{br_0}\right)\right\} - \frac{ac'}{cb^3}\left(\ln f_1 + \frac{ha}{bf_1}\right)_{z=0}\right]$$
$$\left. + g_2\left[\eta - \frac{a}{b^2}r_0 - \frac{h}{b^3}\ln f_0\right]_0^\eta \right\}. \tag{62}$$

The integral in (62) still has two singularities in it, one due to the term $1/h$ and the other due to the term $(\ln f_1)_{z=0}$, since

$$(f_1)_{z=0} = |h| + ha/b \equiv f_{00}, \quad \text{say.}$$

These two singularities are removed in the same way as the corresponding ones in Section 4. At $h = 0$,

$$\frac{r_0 - h}{\eta} - \frac{a^2\eta}{r_0} = b - \frac{a^2}{b} = \frac{1}{b}$$

so a part $g_{0c}/b_c h$ is subtracted to deal with the $1/h$ singularity, and a part $g_{0c}(a_c c'/b_c^3 c)\ln|h|$ is added to deal with the $\ln|h|$ one. Since

$$\int_0^\pi \frac{d\phi}{h} = 0$$

and from (46)

$$\int_0^\pi \ln|h|\, d\phi = \pi\ln(\tfrac{1}{4}c),$$

we must subtract $g_{0c}(a_c c'/b_c^3 c)\pi\ln(\frac{1}{4}c)$ to compensate, and (62) becomes—with a little further rearrangement—

$$\int_0^\pi \left[g_0\left(I_0 - a\frac{\partial I_1}{\partial h}\right) + g_2 I_2\right]_0^\eta d\phi = -4\frac{g_{0c}}{c\sin\phi_c}\left\{ a_c - \frac{1}{b_c}\ln(b_c + a_c)\right\} - g_{0c}\frac{a_c c'}{b_c^3 c}\pi\ln(\tfrac{1}{4}c)$$
$$+ \int_0^\pi d\phi\left\{ \frac{1}{h}\left\{ g_0\left(\frac{r_0 - h}{\eta} - \frac{a^2\eta}{r_0}\right) - \frac{g_{0c}}{b_c}\right\} - g_0\frac{a}{r_0}\right.$$
$$+ \left(g_0\frac{c'}{c}\frac{a}{b^3} - g_2\frac{h}{b^3}\right)\left(\ln f_0 - \ln f_{00}\right) + g_{0c}\frac{c'}{c}\frac{a_c}{b_c^3}\ln|h|$$
$$\left. + g_0\frac{c'}{c}\frac{a}{b^3}\left[\frac{1}{f_0}\left(\frac{ha}{b} - \eta b - \frac{\eta^2 b^2}{r_0}\right)\right]_0^\eta + g_2\left[\eta - \frac{a}{b^2}r_0\right]_0^\eta \right\}. \tag{63}$$

At the control point, where $h = 0$, the first line in the integrand of (63) is dealt with by L'Hospital's rule; the second and third lines contain jump discontinuities at $h = 0$, because $f_{00}/|h|$ does, but these will be integrated correctly by the trapezoidal rule if the mid-point of the jump values is taken. Thus when $h = 0$, the integrand in (63) is replaced by

$$\frac{dg_0/d\phi}{\frac{1}{2}c\sin\phi}\frac{1}{b} + \frac{g_0}{\eta}\left(\frac{a^3}{b^3} - 1\right) + g_0\frac{c'}{c}\frac{a}{b^3}\{a^2 - 2 + \ln(2\eta b^2)\} + g_2\left[\eta - \frac{a}{b^2}r_0\right]_0^\eta \tag{64}$$

evaluated at $\phi = \phi_c$.

6. Loading Representations and Other Details

6.1. Parabola Fitting

Before any spanwise integration can be done, the values of g_0, g_1 and g_2 in the expansion (11) must be known. A typical integration strip contains 3 partition lines, for example the lines A, B, C in Fig. 1, and if $L(\phi, Y)$ is known at 3 points corresponding to a given ϕ, for example the points A', B', C', the parabola is (writing Y_A for the value of Y on the line A, and $L(A')$ for the value of L at the point A')

$$L = L(B') + E(Y - Y_B) + E'(Y - Y_B)^2, \tag{65}$$

where we write

$$Y_C - Y_B = h_1, \qquad Y_A - Y_B = h_2,$$
$$L(C') - L(B') = j_1, \qquad L(A') - L(B') = j_2$$

and

$$E = (j_2 h_1^2 - j_1 h_2^2)/h_1 h_2 (h_1 - h_2),$$
$$E' = (j_1 h_2 - j_2 h_1)/h_1 h_2 (h_1 - h_2).$$

In this case B is the reference line, and carries the value $Y_B = y + \eta^*$ where in general $\eta^* \neq 0$, *see* Fig. 2. Replacing Ys by ηs according to (10), we have for (65)

$$L = L(B') + E(\eta - \eta^*) + E'(\eta - \eta^*)^2$$

whence

$$\left.\begin{aligned} g_0 &= L(B') - E\eta^* + E'\eta^{*2}, \\ g_1 &= E - 2E'\eta^* \end{aligned}\right\} \tag{66}$$

and

$$g_2 = E'.$$

In this way the local expansion about $\eta = \eta^*$ is transformed into one about $\eta = 0$, so that the spanwise integrations can be accomplished for all the strips, and not just the control strip. The reader may enquire whether time and computing effort would be saved by employing a simple panel-type method of integration over the strips other than the control strip, rather than the complicated equations of Sections 4 and 5. The answer is that such a method turns out to be significantly less accurate than analytic integration for several strips on either side of the control strip, typically to about quarter span to port and starboard, and in any case (because of the chordwise refinement, to be discussed later) the control strip takes up more computing time than the other strips. So the analytic method is used, starting with (66), even for the strip shown in Fig. 2.

For such a strip, we remark (perhaps tritely) that $\eta = \eta_-$ would be line A, and $\eta = \eta_+$ would be line C. However, this would not always be true. Consider the situation when the control point is on an 'even' partition line, for example the fourth, counting the centre line as zero (Fig. 4). The integration program always starts from the centre line $\eta = 0$ and works outwards to starboard (after each starboard strip it does the mirror-image port strip also, except when $y = 0$, that is when the control line is the centre line, in which case we take advantage of symmetry of wing and loading and simply double the final answer). So the program begins with the strip (0, 2), the lines 0, 1, 2 corresponding to $\eta = \eta_-, \eta^*, \eta_+$. But it would not normally do the strip (2, 4) next, because line 4 is the control line; we have seen in Section 4 that the control line cannot correspond to $\eta = \eta_+$ or $\eta = \eta_-$ when $z = 0$, and even when $z \neq 0$ we would prefer it otherwise. The different representations of the loading over (2, 4) and (4, 6) could not be expected to join perfectly at line 4; there would be a very slight discontinuity in first spanwise derivative at 4, leading to a very small $\ln z$ term in the computed downwash (physically the discontinuity represents a spurious isobar kink if the planform is well-behaved). So information on lines 2, 3, 4 (corresponding to A, B, C on Fig. 1) is used to compute (66) for each ϕ, but the

integration is done over (2, 3); line 2 becomes $\eta = \eta_-$, line 3 $\eta = \eta_+$. Then we integrate over (3, 5) in the usual way, and avoid spurious discontinuities in the representation at the control line.

The same sort of break would be made if line 3 in Fig. 4 happened to be a kink station; the only difference is that when integrating over (2, 3) information is taken from the lines 1, 2, 3. Thus a slight program restriction is that there must be at least one partition line between any two kink stations or between the centre line and a kink.

We proceed similarly when the control point is on the centre section plane, $y = 0$, but not on the wing plane, so that $z \neq 0$. If the planform is swept, and the isobars are kinked in the physical plane, for instance to maintain the outboard chordwise loading right into the root, the downwash has a real singularity of $\ln z$ type and there is no problem; the program for $z \neq 0$ will evaluate it, including the $\ln z$ behaviour to sufficient accuracy. For this case, the first integration strip is (0, 2). But if the isobars are rounded and we are attempting the evaluation of downwash on the centre line $y = z = 0$, as in Section 5, we need to calculate the second spanwise coefficient g_2 for use in (63). One method we have tried for this is to generate a value of the first spanwise derivative g_1 at the root, with the help of the rounded-isobars condition. With the values of L on $\eta = 0$ and on the first outboard station $\eta = \eta_+$, this gives 3 conditions to determine a quadratic fit across the strip (0, 1).

The rounded-isobars condition $(\partial l/\partial Y)_X = 0$ gives

$$\left(\frac{\partial l}{\partial Y}\right)_\xi = \left(\frac{\partial l}{\partial Y}\right)_X + \left(\frac{\partial X}{\partial Y}\right)_\xi \left(\frac{\partial l}{\partial X}\right)_Y$$

$$= (x_L' + \xi c')\left(\frac{\partial l}{\partial X}\right)_Y \qquad \text{by (12)}$$

$$= a\frac{(\partial l/\partial\phi)_Y}{\frac{1}{2}c\sin\phi} \qquad \text{by (8) and (15).}$$

The value of $(\partial L/\partial Y)_\phi$ is now obtained in terms of $l^* = l\sin\phi$; we have

$$\frac{\partial l}{\partial\phi} = \frac{1}{\sin\phi}\frac{\partial l^*}{\partial\phi} - \frac{\cos\phi}{\sin^2\phi}l^*$$

and so

$$\left(\frac{\partial L}{\partial Y}\right)_\phi = \frac{\partial}{\partial Y}\{c(Y)l(\phi, Y)\sin\phi\}$$

$$= c'l^* + c\sin\phi\frac{a(\partial l/\partial\phi)_Y}{\frac{1}{2}c\sin\phi}$$

$$= c'l^* + 2a\left(\frac{1}{\sin\phi}\frac{\partial l^*}{\partial\phi} - \frac{\cos\phi}{\sin^2\phi}l^*\right). \tag{67}$$

And this is the value of E to use in (65) on the centre line. Hence

$$g_2 \equiv E' = [L(C') - L(B') - EY_1]/Y_1^2. \tag{68}$$

At the leading and trailing edges, (67) breaks down. However, at the trailing edge $\phi = \pi$, $l \equiv 0$ (by the Kutta condition) and so $E = E' = 0$ and there is no problem.

We remark that l^* is a more convenient function to work with than l because, like L, it is usually well-behaved in $0 \leqslant \phi \leqslant \pi$; see the discussion under (9). In particular, $\partial l^*/\partial\phi$ is more amenable to numerical calculation than $\partial l/\partial\phi$ which is unbounded as $\phi \to 0$. However, because in general $\partial l^*/\partial\phi$ would have to be computed numerically (with consequent small error) the question arises whether defining E by (67) on the centre line would indeed ensure no spurious logarithmic behaviour in the downwash.

In fact, in a region of the apex of a swept wing, this value of E is rather sensitive to the accuracy with which $\partial l^*/\partial\phi$ is calculated, and to the position of the other datum point at η_+; since in general $\partial l^*/\partial\phi$ will not be known analytically, and a 4-point central difference formula would place a heavy strain on the smoothness of the data, we must be content with a 2-point central difference formula for $\partial l^*/\partial\phi$ and hope we have a sufficiently close computing mesh in both directions. If the spanwise mesh is close, we can also try linear extrapolation of g_2 from the ordinary values calculated on the first two outboard partition lines. After many

numerical experiments with the swept wing discussed in the next section under Results, we have found that the method using the analytic value of $\partial l^*/\partial\phi$ gave the best results and the extrapolated values of g_2, the worst, compared with another computer solution; so in that section we have given the results with the 2-point central difference values, these being normally the best available.

This behaviour highlights an important deficiency in the program. Near the apex of a swept wing, a line of constant ϕ would be roughly parallel to the starboard leading edge, approaching the centre line from the starboard side; if this line were extrapolated to the port side it would cut the port leading edge at a point P which would be very close to the centre line for centre line points near the apex. Since this point P on the port wing carries a loading singularity, the circle of convergence of a power series for our function L about $(\phi, 0)$ cannot extend beyond P, and so the region in which our three-term representation of L is valid becomes very small as the apex is approached. Mathematically our technique is not valid, and for computing purposes we need to take a fine spanwise partitioning (to keep the contribution to the chordwise integral from the wrongly treated region as small as possible) to calculate downwash at all reliably on the centre line. One way in which this snag manifests itself is in the sensitivity of g_2 to which we have referred above.

We turn now to a difficulty which arises when integrating up to the wing tips. Without loss of generality we may scale the wing with respect to the semi-span so that the tips are at $Y = \pm 1$. Near the tips the loading is usually elliptic[2] and so

$$L = 0[(1 - Y^2)^{\frac{1}{2}}] \qquad \text{near } Y = \pm 1. \tag{69}$$

It follows that $\partial L/\partial Y$ is unbounded near the tips, and so L cannot be well represented by parabolas near the tips. Unfortunately the present method is geared to representation by parabolas; a proper representation of L leads to elliptic functions which we aim to avoid: so we seek a representation which is a best fit, in the least squares sense, near the tips, and use it over the last interval $(m - 1, m)$ where m is the number of outboard partition lines. This will be better than the usual 3 point fit over $(m - 2, m - 1, m)$ but it will not be perfect, so we aim to make the last interval as small as possible by using a variable partition spacing spanwise as shown in Fig. 1. For example, we might use the Multhopp[1] distribution

$$Y_k = \sin(k\pi/2m), \qquad k = 0(1)m.$$

When the control line is well inboard, the error from the integration over $(m - 1, m)$ is very small. If the control line is actually the line $m - 1$, the error is comparatively large, but we can diminish it by interpolating more partition lines between control line and tip, and interpolating for L on these lines using (69).

By shifts of origin and scale, the problem can be turned into a universal problem of finding the best parabola fit in $0 \leqslant \hat{x} \leqslant 1$ to the function

$$\hat{y} = \hat{x}^{\frac{1}{2}}.$$

We can weight the fit suitably, to match it to the rest of the curve in $\hat{x} \geqslant 1$, by demanding that the parabola pass through (1, 1). The most general such parabola (with axis vertical) is

$$\hat{y} = a\hat{x}^2 + b\hat{x} + (1 - a - b). \tag{70}$$

Minimising the integral

$$\int_0^1 \{(a\hat{x}^2 + b\hat{x} + 1 - a - b) - \hat{x}^{\frac{1}{2}}\}^2 \, d\hat{x}$$

leads to

$$a = -\tfrac{10}{21} = -0{\cdot}4761905$$
$$b = \tfrac{272}{210} = 1{\cdot}295238.$$

The two $(\hat{x}, \hat{y})$ curves are shown in Fig. 5. The overall fit is quite good, the average error in $\hat{y}$ being about 0·02, but the difference in slopes at (1, 1) is sufficient to ruin the calculation of downwash on the line $m - 1$ (corresponding to $\hat{x} = 1$).

From (70), near the starboard tip the parabolic fit to L taking the value $L(B')$ at the point $B'(\phi, Y = Y_{m-1})$ is

$$\frac{L}{L(B')} = a\left(\frac{1 - Y}{1 - Y_{m-1}}\right)^2 + b\left(\frac{1 - Y}{1 - Y_{m-1}}\right) + (1 - a - b)$$

so that

$$E = -\frac{L(B')}{1 - Y_{m-1}}(2a + b) = -0{\cdot}342857\frac{L(B')}{1 - Y_{m-1}}$$

$$E' = a\frac{L(B')}{(1 - Y_{m-1})^2} = -0{\cdot}4761905\frac{L(B')}{(1 - Y_{m-1})^2}$$

Near the port tip $Y = Y_{-m} = -1$ the same value of E' is used (with $Y_{-m+1} + 1$ in place of $1 - Y_{m-1}$; the same thing if the partitioning is symmetrical about the centre line) but the sign of E is changed.

6.2. Chordwise Refinement

From the discussion of Section 4 it is clear that when z is small α_1 as given by (17) will exhibit large chordwise variations on and near the control strip. When $z = 0$, α_1 contains two singularities, which are removed to leave a more tractable function α_0; when z is small but non-zero, these singularities disappear mathematically but two sharp turning points appear instead and these need accurate definition before numerical integration can be attempted.

Referring to (16), let us write

$$A_1 = \alpha_1(\eta_+) - \alpha_1(\eta_-).$$

From the present viewpoint, A_1 is a function of ϕ. Figure 6 shows the typical chordwise behaviour of A_1; the control point, where $h = 0$, is assumed to be at the mid chord point R, and the range $0 \leqslant \phi \leqslant \pi$ has been divided into 16 equal intervals at $A, B, \ldots$ at which l (and hence L) is supposed given. The height and steepness of the peaks depend on z, but $z = 0{\cdot}005$ (for unit semi-span) is representative of the scales shown. Clearly the chordwise integral cannot be determined accurately from just the values of A_1 at $A, B, \ldots, Q, R, S, \ldots$.

So the range is divided into three sub-ranges by setting markers usually 1 or 2 points away from the control point on either side; the best number P' of points to use depends on z and on the number of chordwise points overall, but P' must be at least one. If $P' = 1$, the markers are at Q and S in Fig. 6. The integral from Q to S is calculated by trapezoidal rule using the data points Q, R, S and again using every other data point, in this case just Q, S. If the results do not agree to within a specified tolerance, ε say, then extra points are taken at the mid points of the existing intervals, say at Q_1, R_1 in the inset of Fig. 6; L is interpolated to the corresponding values of ϕ on each partition line, A_1 is calculated at the newly added points and a better value of the integral is obtained. The process is repeated until successive values differ by the required tolerance.

Although this technique is particularly useful near the control point, there is nothing to prevent it being used to refine the integrals for the outer sub-ranges. In general, different levels of refinement are required for all 3 sub-ranges. A_1 tends to be small in the trailing edge sub-range (from S to $\phi = \pi$) for two reasons. First, l decreases towards the trailing edge. Second, consider the last factor of the kernel in (7). When $|X - x| \gg |Y - y|$, we have

$$1 - (X - x)/r \doteqdot 1 - \operatorname{sgn}(X - x) = \begin{cases} 0 & (X > x) \\ 2 & (X < x). \end{cases}$$

So the kernel (and hence A_1) is much smaller far downstream of the control point, as illustrated in Fig. 6, and this sub-range needs less refinement.

We can apply this method to all the integration strips. There are roughly m of these strips, and in general we deal with three sub-ranges in each, so by (16) the maximum error in α would be $(3m\varepsilon)/16\pi$. If we need at least three decimal places accuracy ($3D$) in α, this gives

$$\varepsilon \doteqdot 0{\cdot}017/m.$$

In practice the errors are not cumulative, and much smaller outboard of the control strip, and this tolerance gives at least $4D$ accuracy.

If the control point is near (within P' points of) the leading or trailing edges, one sub-range disappears and there are only 2 sub-ranges to integrate over, in each strip.

The next question is, how is L to be interpolated on the partition lines. At first, it was thought that linear interpolation between neighbouring points, with a quadratic interpolation at the leading and trailing edges,

would be good enough; for flat plate loading, the function L behaves chordwise like $(1 + \cos\phi)$ and with 16 chordwise datum points a typical error in the downwash is 0·5 per cent. However, if higher Fourier components are introduced into the chordwise loading, the errors can rise to upwards of 1 per cent. A quadratic chordwise interpolation rule was next tried, using information typically from points $(p - 1, p, p + 1)$ to interpolate between points $(p, p + 1)$, and on average the errors were roughly halved using this rule. But it is a one-sided rule, it is unsymmetrical and does not produce an arcwise smooth interpolate, and so we have developed a rule which does produce an interpolate with a continuous first derivative. To do this, we prescribe the values of the first derivative at each data point, requiring that these values equal the 2-point central difference values, which would be obtained by a quadratic through $(p - 1, p, p + 1)$:

$$\left(\frac{\partial L}{\partial \phi}\right)_p = (L_{p+1} - L_{p-1})/2A$$

(A being the steplength). In the range $(p, p + 1)$ this gives 2 conditions to be satisfied at each end, so a cubic is fitted to the 4 conditions, and the complete set of cubics defines the chordwise interpolate. It is not a cubic spline interpolate as the second derivatives are discontinuous in general, but it is simpler and quicker to generate than a cubic spline. For the cases mentioned above, still further improvement in accuracy is obtained.

The first derivatives are set to zero at the leading and trailing edges. This avoids theoretical logarithmic singularities in the integration near these points, away from the root.

Finally, it is possible to calculate the downwash at the leading and trailing edges (except the apex of a swept wing), by making the following provisions. At the trailing edge, the factor (g_{0c}/h) in (48) or (63) is replaced by its L'Hospital equivalent, and at both leading and trailing edges $(\phi = 0, \pi)$ the factor

$$\frac{dg_0/d\phi}{\sin\phi}$$

in (50) or (64) is replaced by its L'Hospital equivalent

$$\left[\frac{d^3g_0/d\phi^2}{\cos\phi}\right].$$

The second derivative is calculated from a 3-point rule consistent with the cubic interpolate; it must be consistent, otherwise the chordwise integrand will be discontinuous and the chordwise refinement necessary to overcome this will increase computing times unacceptably.

7. Examples

7.1. Unyawed Infinite Flat Plate

As a first check on the program, we consider the two-dimensional flow over a flat plate of constant (unit) chord and infinite span. An exact solution is available in linearized theory; if the incidence is $\frac{1}{4}$, the load distribution (which is independent of Y, of course) is

$$l(X) = (1/X - 1)^{\frac{1}{2}}.$$

Inserting into (7) and performing the spanwise integration, we have

$$\alpha = \frac{1}{4\pi}\int_0^1 \frac{(1/X - 1)^{\frac{1}{2}}(x - X)\,dX}{(x - X)^2 + z^2}.$$

Putting successively $X = \sin^2\psi$, $\tan\psi = t$, we find

$$\alpha = \frac{1}{4} - \frac{1}{2\pi}\int_0^\infty \frac{t^2 - a}{t^4 - 2at^2 + b}dt$$

where (for this section only) we write

$$a = \frac{x(1 - x) - z^2}{(1 - x)^2 + z^2}, \qquad b = \frac{x^2 + z^2}{(1 - x)^2 + z^2}.$$

With

$$c = (b - a^2)^{\frac{1}{2}} = \frac{z}{(1-x)^2 + z^2} > 0$$

we have

$$\alpha = \frac{1}{4} - \frac{1}{2\pi}\int_0^\infty \frac{t^2 - a}{(t^2 - a)^2 + c^2}\,dt$$
$$= \frac{1}{4} - \frac{1}{2\pi}\mathrm{Re}\int_0^\infty \frac{dt}{t^2 - (a + ic)}$$

which can be evaluated by contour integration:

$$\alpha = \frac{1}{4} - \frac{1}{4}\mathrm{Re}\frac{i}{d + ie} = \frac{1}{4} - \frac{1}{4}\frac{e}{d^2 + e^2}$$

where

$$(d + ie)^2 = a + ic, \qquad e > 0$$

whence

$$e^2 = \tfrac{1}{2}(\sqrt{a^2 + c^2} - a) = \tfrac{1}{2}(\sqrt{b} - a)$$
$$d^2 + e^2 = \sqrt{a^2 + c^2} = \sqrt{b}$$

and so

$$\alpha = \tfrac{1}{4} - \tfrac{1}{4}[\tfrac{1}{2}(\sqrt{b} - a)]^{\frac{1}{2}}/\sqrt{b}. \tag{71}$$

On the flat plate $z = 0$, $a^2 = b$, and $\alpha = \frac{1}{4}$, as it should. The analytic solution is thus known for the flat plate of infinite aspect ratio.

The computer program for $z \neq 0$ was run, at fixed $(x/c, z/c)$ positions on the centre section of a rectangular wing with flat plate loading, constant along the span, for various values of aspect ratio AR. Positions near the leading edge were chosen, as the downwash varies quite rapidly there. Figure 7 shows the downwash at each position, as a function of $1/AR$, along with the values from (71) for infinite AR, and we see that all points for each position lie exactly on parallel straight lines, to within graphical accuracy (3D). We can see how this comes about, as follows. The difference in downwash for finite and infinite wings with constant spanwise loading is chiefly due to the concentrated trailing vortex shed from each wing tip on the finite wing; for points on the centre section these two semi-infinite vortices are roughly equivalent to a single two-dimensional vortex of the same strength ΓU, where $\Gamma = \frac{1}{2}\pi c C_L = \frac{1}{4}\pi c$, and so induce an extra downwash

$$\frac{\Gamma}{2\pi s} = \frac{\frac{1}{4}\pi c}{2\pi s} = \frac{1}{4AR}$$

so that

$$\frac{\partial \alpha}{\partial(1/AR)} = \frac{1}{4},$$

independently of position, and hence the parallel lines, which in Fig. 7 have slopes around 0·258 to 0·260.

As further evidence, we draw attention to the three points for $AR = 24$, $x/c = 0{\cdot}0955$; since the difference between results $z/c = 0{\cdot}012$, 0·006 is just twice that for $z/c = 0{\cdot}006$, 0·003, the linear variation of downwash with z near the plate (which can be analytically predicted for $z \ll x$, $z \ll 1 - x$) is also verified. For these calculations, 20 chordwise stations and $m = 10$ spanwise stations were used to specify the loading.

7.2. Rectangular Wing with Elliptic Loading

We next consider a rectangular wing, which being unswept will not incur the problems associated with the apex of a swept wing. We take the aspect ratio to be 6 and impose a flat-plate chordwise and elliptic spanwise loading

$$l = (c/x - 1)^{\frac{1}{2}}(1 - y^2/s^2)^{\frac{1}{2}}.$$

To get some idea of the numbers expected from classical aerofoil theory, we observe that the section lift coefficient

$$C_L(y) = \tfrac{1}{2}\pi(1 - y^2/s^2)^{\frac{1}{2}}$$

and then Prandtl's classical aerofoil equation[3] gives

$$\begin{aligned}\alpha(y) &= \alpha_e + \alpha_i \\ &= \frac{C_L(y)}{2\pi} + \frac{1}{8\pi}\int_{-s}^{s} \frac{d(cC_L)}{dy'}\frac{dy'}{y - y'}.\end{aligned}$$

This result can be derived from the assumption

$$|X - x| \ll |Y - y| \tag{72}$$

in equations (5) and (7), for $z \to 0$.

Substituting for C_L, and putting $y = 0$, we find

$$\alpha_e = 0{\cdot}25$$

and

$$\alpha_i = (c/s)(\pi/16) = 0{\cdot}06545 \qquad \text{(aspect ratio = 6).}$$

α_e is just the flat-plate downwash on an infinite wing with two-dimensional chordwise loading, while α_i is a measure of the contribution from the trailing vortex system. From the assumption (72) it follows that α_i is independent of x and is just half its value in the wake where the vortices are effectively infinite upstream and downstream. This leads to the value $\alpha = \alpha_e + \alpha_i = 0{\cdot}315$. For a finite wing, α_i is rather more than half its wake value, so in the R.A.E. standard method it is multiplied by a downwash factor[3] ω with a value between 1 and 2. For aspect ratio 6, $\omega = 1{\cdot}026$ and

$$\alpha = \alpha_e + \omega\alpha_i = 0{\cdot}317,$$

so the classical treatment gives a value of $\alpha = 0{\cdot}317$ on the centre line. How well this approximation is confirmed is shown in Fig. 8, in which this result is compared with calculations due to Garner,[7] reported also by Freestone.[5]

We observe that, for this particular unswept wing, the assumption (72) with the incorporated downwash factor together produce an error of about 4 per cent in trailing-edge downwash; that there is an error at all here is entirely due to the aspect ratio being finite (6) rather than infinite.

Using the program for $z \neq 0$, at each chordwise station the downwash was calculated for two suitably small values $z/c = 0{\cdot}0015$ and $0{\cdot}0030$, and the results are also shown in Fig. 8. Since the isobars are perfectly smooth at the centre line, we again expect the downwash to be partly constant and partly proportional to z, and indeed (except at the last point, $x/c = 0{\cdot}975$, before the trailing edge) the points for $z/c = 0{\cdot}0015$ lie halfway between the Garner curve and the points for $z/c = 0{\cdot}0030$, at the same x/c. Thus the program is again indirectly verified. The effect near the leading edge is startling considering the large difference involved; it comes about because although the downwash on $z = 0$ remains finite as $x \to 0+$, the downwash on $x = 0$ is unbounded as $z \to 0+$. (It is readily verified from (71) for the previous problem that the downwash is $0(z^{-\frac{1}{2}})$.) This non-uniform behaviour, as the same point is approached from different directions, is a consequence of linear theory and the thin-wing assumption; it affects the calculations considerably very near the leading edge, as Fig. 8 shows.

The downwash computed on the centre line by the method of Section 5 is also shown in Fig. 8, including the leading edge $x/c = 0$ and the trailing edge $x/c = 1$, and we see that the values all agree with those from Garner's theory to within the three figures of graphical accuracy.

For interest, the centre-line warp

$$\frac{z(x/c)}{c} = \int_{x/c}^{1} \alpha(x')\, dx'$$

is computed and results from present method and R.A.E. standard method are shown in Fig. 9. We see that the assumptions of the R.A.E. method (as above) produce an error of about 3 per cent at $x/c = 0{\cdot}3$, for this unswept wing.

7.3. Swept Constant Chord Wing

To demonstrate the program's operation on a kinked isobar configuration, we take a swept wing of constant chord with straight leading edges port and starboard, so that each half of the planform is a parallelogram, and impose flat-plate loading on it as for the unswept wing of Section 7.1, with constant spanwise loading:

$$l(X) = (1/X - 1)^{\frac{1}{2}}.$$

Wings with 45 degrees sweepback and aspect ratios of 6, 12 and 24 were studied. Sixteen chordwise stations were used. With the aspect ratio 6, the chordwise downwash distribution at the centre line is shown in Fig. 10 for $z/c = 0{\cdot}005$ and $0{\cdot}010$. Also shown, is the flat plate chordwise downwash distribution on a yawed infinite straight wing carrying the same loading, which distribution would also be expected on a section of our finite wing, far outboard but not near the tip. For this case, on $z = 0$ the spanwise integration yields

$$\begin{aligned}(\alpha)_{\text{yawed wing}} &= (\alpha)_{\text{unyawed wing}}\, b \\ &= 0{\cdot}25\sqrt{2} = 0{\cdot}354.\end{aligned}$$

The figure thus shows the sort of extra reverse camber needed to maintain the same load distribution at the centre section of this swept wing; it depends on z but certainly no longer has flat plate character. We also notice in passing that for the larger value of z/c the downwash dips sharply as we approach the apex, which is the same effect as before: there is a region of strong upwash just above the leading edge.

From the results for these three aspect ratios, we may again extrapolate to the infinite wing just as for the unswept case. The results for three near-mid-chord stations are shown in Fig. 11 (the vertical scale has been stretched and broken up, as there is very little difference between the results on the scale of Fig. 10). We also show theoretical results for the infinite wing, computed from the formula:[6]

$$\begin{aligned}\alpha(x, 0, z) &= \frac{b}{4\pi}\int_0^1 \frac{l(X)(x - X)\, dX}{(x - X)^2 + z^2b^2} + \frac{a}{4\pi}\int_0^1 \frac{l(X)\, dX}{[(x - X)^2 + z^2]^{\frac{1}{2}}} - \frac{a}{4\pi}\int_0^1 \frac{l(X)\, dX}{[(x - X)^2 + z^2]^{\frac{1}{2}}} \frac{z^2b^2}{(x - X)^2 + z^2b^2} \\ &= K_1 + K_2 + K_3.\end{aligned}$$

This expression also follows from Section 3, with $g_1 = g_2 = 0$ but $a \neq 0$. K_1 comes from the limit $\eta = \infty$ in the spanwise integration; it is analogous to the two-dimensional flat-plate result of Section 7.1 and can be dealt with similarly by replacing z by zb and finally multiplying by b. Also, when $x = 0$, K_1 is again $0(z^{-\frac{1}{2}})$ as $z \to 0+$, which dominates K_2 and K_3 and accounts for the strong upwash field near the apex. K_2 and K_3 come from the limit $\eta = 0$, and for our flat-plate loading they are elliptic integrals. These were not manipulated into standard forms but evaluated directly by trapezoidal integration with 256 points in a check program; the results are nearly identical with the extrapolated values from the main program, as the four points for each station are nearly collinear. Similar agreement was found elsewhere, except near the leading edge where the accuracy of the check program fell off. This could be improved by taking more than 256 points, but it is a very minor detail.

The logarithmic singularity in the downwash for kinked isobars as $z \to 0$ comes from the integral K_2. For $z, z_1 \ll x, 1 - x$, K_2 gives

$$\alpha(x, 0, z) - \alpha(x, 0, z_1) \sim (a/2\pi)l(x) \ln (z_1/z).$$

So near the mid-chord we expect the function

$$\chi = \frac{\alpha(x, 0, z) - \alpha(x, 0, z_1)}{(a/2\pi)l(x) \ln (z_1/z)}$$

to be approximately 1. The table below shows the chordwise variation of χ and confirms this expectation.

x/c	0·0381	0·1464	0·3087	0·5000	0·6913	0·8536	0·9619
χ	1·324	1·100	1·056	1·047	1·055	1·094	1·302

Near the leading edge, K_2 gives precedence to K_1 which has the stronger singularity.
Similar reasoning to that for the unswept wings of Section 7.1 leads to the approximate result

$$\frac{\partial\alpha}{\partial(1/AR)} = \frac{1}{4}\left(1 - \sin\frac{\pi}{4}\right) = 0{\cdot}073.$$

The values from Fig. 11 are 0·073, 0·080, 0·083, in good agreement.

7.4. Swept Wing 'A'

Wing A has a swept planform with straight leading and trailing edges to port and starboard, streamwise tips, aspect ratio 6, taper ratio $\frac{1}{3}$ and midchord sweep angle 30 degrees. Thus, for unit semi-span, the leading edge and chord are given by

$$x_L = 0{\cdot}7440168\,Y$$

and

$$0 \leqslant Y \leqslant 1.$$

$$c = 0{\cdot}5 - 0{\cdot}3333333\,Y$$

As a mutual check on their individual programs, M. M. Freestone[5] and the author assumed flat-plate chordwise loading and elliptic spanwise loading with an overall lift coefficient $C_L = 1$:

$$l(\xi, Y) = \frac{8}{3\pi^2}\left(\frac{1-\xi}{\xi}\right)^{\frac{1}{2}}\frac{(1-Y^2)^{\frac{1}{2}}}{c(Y)}.$$

Freestone used a 15 (chordwise) × 20 (spanwise) rectangular grid in the physical plane, while the author used a 20 × 20 grid with uniform spanwise spacing. This is contrary to the decision of Section 6.1; the program was still being developed. Thus calculations near the tip would have been useless, but good results were still expected well inboard.

The isobars are now kinked at the centre line, so the downwash cannot be calculated there for $z = 0$. Instead comparisons were made at two sections well inboard, $Y = 0{\cdot}05$ and 0·1, and one section near mid-span, $Y = 0{\cdot}4$, and are shown in Fig. 12. (The author's results were originally extrapolated from those for 3 values of $z \neq 0$, but the program for $z = 0$ gave exactly the same results. Thus the present work really does verify this latter program.) The overall agreement is good, particularly for $Y = 0{\cdot}4$ where the camber section is virtually a flat-plate. A closer examination reveals that for the inboard sections $Y = 0{\cdot}05$ and 0·1 the Freestone values show some oscillation along the chord about the author's comparatively smooth curve, and for $Y = 0{\cdot}4$ one Freestone value, for a point quite near the leading edge, lies well below the general straight line. It is thought that Freestone's program (which has a fixed number of grid refinements for each point, set in advance by the programmer) did not refine sufficiently for this point, and that further refinement would have considerably improved this value; however, it is also thought that Freestone's grid, which does not follow the contours of swept planforms, may introduce some integration errors at the edges which are responsible for the oscillatory behaviour. This can even be important near the trailing edge (where the chord loading is small), as the values there show in Fig. 12 (for the inboard section). The author's program trades this defect against analytical complexity, apparently with profit.

7.5. Special Delta Wing

No proper test of the method for thin swept wings was available at the time of writing. A load distribution obtained by Multhopp's collocation method[2] cannot be used as this method depends on first rounding the apex. So an artificial case was chosen to check the program further. An analytic load distribution was chosen to give a square-root (not inverse square-root) singularity along the leading edges of a 45 degree delta wing (the root chord thus being equal to the semi-span), and to go to zero at the trailing edge. The actual trailing-edge behaviour was chosen quadratic, for the following reason. It is possible to specify the wing instead as a constant

chord wing, still with 45 degree sweep, with only the triangle loaded, and to repeat the calculations for this wing as a check, both on and off the centre line. For the constant chord model, the local sweep a will be everywhere constant and the spanwise rate of change of chord c' will be zero; for the triangular model, a will vary along the chord and c' will here be equal to -1. For self consistency the results must agree even though all the numbers in the arithmetic will be different. Now if the normal trailing edge behaviour is chosen, then on the constant model the function L will have a sharp change of slope on a chordline outboard of the centre line, and the chordwise interpolation routine will produce results which depend on where the data points are. A quadratic variation must be chosen to fair smoothly into the region of zero loading behind the triangle. A factor 10 was inserted to obtain downwash values in the range 0 to 1, and the analytic formula chosen was thus

$$l(x, y) = 10(x^2 - y^2)^{\frac{1}{2}}(1 - x)^2.$$

The computed distribution of downwash both on and off the centre line is shown in Fig. 13. Thirty-two chordwise points were used, as this run was done before the cubic interpolation technique had been decided on. Values at each of three stations near the centre line were calculated using both models; the same values of ϕ lead to different values of the physical coordinate x when $y \neq 0$ so the points obtained are different but all lie on the same curve (except perhaps the last point on the station $y = 0{\cdot}05$). This is not important as it does no more than verify the consistency of Section 4. Now, when $y = 0$ the control points are the same for both models, and the results of the two calculations (also shown in the table below) agree to 3 decimal places and cannot be distinguished on the graph. This verifies the consistency of the present method.

x	0·0381	0·1464	0·3087	0·5000	0·6913	0·8536	0·9619	1·0
Constant chord wing	−0·0705	0·1293	0·4578	0·7564	0·9036	0·9101	0·8729	0·8584
Triangular wing	−0·0707	0·1291	0·4579	0·7564	0·9029	0·9093	0·8730	0·8589

Moreover, we see from the figure that the curve for $y = 0$ is within a reasonable extrapolation region of the three curves shown for $y \neq 0$.

On Fig. 13 we also show downwash values obtained from the corresponding program of Freestone.[4] These are consistently higher than our values, and the differences are larger than one would expect from the comparison reported in Section 7.4 with Fig. 12, so if Freestone's results (obtained using a 20 × 20 Cartesian grid with refinement) are accepted as near accurate, then our results are perhaps a maximum of 2 per cent in error. As discussed in Section 6, our computation is sensitive to the method used for calculating g_2; we can improve the accuracy by using analytic or high-order difference approximations for $\partial l^*/\partial\phi$ on the centre line, but these resources are not normally available and so the calculation would not be representative. Meanwhile, the present results give an estimate of the likely error using this particular partition line spacing ($y/c = 0$, 0·025) for our 45 degree swept wing.†

8. Concluding Remarks

We now have two programs which use as data the planform shape and steady loading distribution at points on a planform grid, and calculate the downwash derived from linear theory; one program for points on the planform with $z = 0$, the other for points off it with $z \neq 0$. The storage requirements are not high, as not much more is required than is needed for the above data, though the analytic complexity is considerable; in these days of high speed computers the number of function evaluations in the chordwise refinement scheme causes no alarm; the accuracy of the output depends primarily on the denseness of the input and is quite acceptable, for the cases considered in this Report, with only 16 × 20 or so input numbers.

The program for $z \neq 0$ has obvious uses. The designer may specify a straight isobar configuration with mathematical kinks at the centre section of a swept wing. In thin wing theory this leads to the impossible situation of infinite downwash on the centre section $y = z = 0$; but in practice the wing always has a finite

† Since the writing of the above, the author has tried the program on the centre line of a flat cropped delta wing with a loading calculated by the method of Hewitt,[8] including the apex eigensolutions found by Rossiter.[9] The author failed to obtain consistent results, and concludes that for such loadings his program is in fact inadequate on the centre line of a swept wing.

thickness distribution, and so we can escape with a computation of downwash on the thick wing which, compounded with the velocity component due to thickness only, gives a possible design centre section. Another possible application is the design of wing-fuselage combinations for given load distribution, when similar programs for the calculation of the other induced velocity components are required.

The program for $z = 0$ could also serve as a design tool, perhaps the most accurate to date of its kind. Moreover, there is doubt about the accuracy of the collocation methods (at points other than collocation points) for the loading problem,[4] and there are some challengeable assumptions in the R.A.E. standard method;[3] these points may be clarified by a direct check with the program, as has recently been done by Weber.[10]

The program can also attempt to compute the downwash on the centre line $y = z = 0$—with qualifications. For wings without centre line sweep (for instance, rectangular wings) there seems to be no problem; for swept wings, a grave mathematical difficulty arises at the apex and a close mesh spacing is required to obtain numerical results in which we may have any confidence, even though an excellent self-check has been obtained for the special wing discussed in Section 7.5. At the moment this difficulty has not been tackled.

Finally, we mention that the downwash can be calculated both at leading and at trailing edges (except at the apex of a swept wing), but not at the wing tips, because of the fictitious way the loading is represented there. But it is doubtful whether this last restriction matters much in practice, as there is always the shed wing tip vortex to contend with.

LIST OF SYMBOLS

AR	Aspect ratio
A_1	$\alpha_1(\eta_+) - \alpha_1(\eta_-)$
a	Local sweep, $x'_L + c'\xi$
b	$\sqrt{(a^2 + 1)}$
$c, c(Y)$	Chord
c'	$dc(Y)/dY$
f	$r + \eta b + ha/b$
g_0, g_1, g_2	Coefficients in expansion of L about control line: $L(\phi, Y) = g_0 + \eta g_1 + \eta^2 g_2$
h	$x^*_L + c^*\xi - x$; defined by $X - x = h + \eta a$
$\hat{I}$	Indefinite integral over spanwise strip, *see* (18)
$\hat{I}_0, \hat{I}_1, \hat{I}_2$	$\hat{I} = g_0\hat{I}_0 + g_1\hat{I}_1 + g_2\hat{I}_2$
I_0, I_1, I_2	$I_p = \partial\hat{I}_p/\partial z$
l	Wing load distribution
l^*	$l \sin\phi$
L	$l(X, Y)c(Y) \sin\phi$
r	$r^2 = (X - x)^2 + (Y - y)^2 + z^2$ $= (h + \eta a)^2 + \eta^2 + z^2$
s	Semispan
U	Freestream velocity
x, y, z	Cartesian coordinates of point where downwash is being evaluated
X, Y	Cartesian coordinates of point in wing plane
$x_L, x_L(Y)$	leading edge X coordinate
x'_L	$dx_L(Y)/dY$
α	Downwash
α_1	$\partial\hat{I}/\partial z = g_0 I_0 + g_1 I_1 + g_2 I_2$
Δ	Potential jump across wing plane $= \frac{1}{2}U\Delta$; $l = \partial\Delta/\partial x$
ϕ	Chordwise angular coordinate; $\xi = \frac{1}{2}(1 - \cos\phi)$
ξ	Local section coordinate; $X = x_L(Y) + \xi c(Y)$
η	$Y - y$; spanwise coordinate measured from control line
η_-, η_+	Limits of spanwise integration strip
η^*	Reference point for expansions, $\eta_- \leqslant \eta^* \leqslant \eta_+$
Subscripts	
0	On f, r; values when $z = 0$
1	On f, r; values when $\eta = 0$
c	Values when $h = 0$ (control point)

REFERENCES

No.	Author(s)	Title, etc.
1	H. Multhopp	Methods for calculating the lift distribution of wings (subsonic lifting surface theory). A.R.C. R. & M. 2884 (1950).
2	B. Thwaites	*Incompressible aerodynamics.* Chapter VIII, Clarendon Press (1960).
3	D. Küchemann	A simple method for calculating the span and chordwise loading on straight and swept wings of any given aspect ratio at subsonic speeds. A.R.C. R. & M. 2935 (1952).
4	H. C. Garner	Numerical appraisal of Multhopp's low-frequency subsonic lifting-surface theory. A.R.C. R. & M. 3634 (1968).
5	M. M. Freestone	Numerical evaluation of singular integrals of linearized subsonic wing theory. A.R.C. 29 729 (1967).
6	J. Weber	The shape of the centre part of a swept-back wing with a required load distribution. A.R.C. R. & M. 3098 (1957).
7	H. C. Garner and G. F. Miller . .	Analytical and numerical studies of downwash over rectangular planforms. *Aeronautical Quarterly*, XXVIII, p. 169 (1972).
8	B. L. Hewitt and W. Kellaway . .	Developments in the lifting surface theory treatment of symmetric planforms with a leading edge crank in subsonic flow. B.A.C. Report No. Ae.313, A.R.C. 33 412 (1971).
9	P. J. Rossiter	The linearized subsonic flow over the centre section of a lifting swept wing. A.R.C. R. & M. 3630 (1969).
10	J. Weber	Notes on the approximate solution of lifting surface theory used in the R.A.E. Standard Method. R.A.E. Technical Report 73044 (1973).

APPENDIX

The Computing Formulae for Streamwash and Sidewash

The potential per unit free stream has been derived in Section 2 as

$$\varphi(x, y, z) = \frac{z}{8\pi} \iint_{\text{wing}} \frac{l(x, Y)}{(Y - y)^2 + z^2} \left[1 - \frac{X - x}{r}\right] dX\, dY \tag{A-1}$$

and the velocity components of $\nabla\varphi$

$$u_l = \frac{\partial\varphi}{\partial x}, \qquad v_l = \frac{\partial\varphi}{\partial y}, \qquad w_l = \frac{\partial\varphi}{\partial z}$$

can also be written as double integrals over the wing planform. The downwash $\alpha = -w_l$ has been considered in the main text, and we have to deal similarly with the streamwash u_l and sidewash v_l in the case $z \neq 0$.

By the method of Section 3, (A-1) is transformed first to a sum of strip integrals similar to (9)

$$\varphi(x, y, z) = \frac{1}{8\pi} \sum_{\text{strips}} \frac{1}{2} \int_0^{\pi} d\phi \,.\, z \int_{\text{strip}} dY \,.\, \frac{L(\phi, Y)}{(Y - y)^2 + z^2} \left[1 - \frac{X - x}{r}\right] \tag{A-2}$$

and then, making use of equations (10), (11) and (15), we have (A-2) in the form similar to (16)

$$\varphi = \frac{1}{8\pi} \sum_{\text{strips}(\eta_-, \eta_+)} \frac{1}{2} \int_0^{\pi} d\phi [\hat{I}(\eta_+) - \hat{I}(\eta_-)] \tag{A-3}$$

where, as (18)

$$\hat{I} = z \int d\eta \, \frac{g_0 + \eta g_1 + \eta^2 g_2}{\eta^2 + z^2} \left[1 - \frac{h + \eta a}{r}\right] = g_0 \hat{I}_0 + g_1 \hat{I}_1 + g_2 \hat{I}_2 \tag{A-4}$$

with

$$r^2 = (h + \eta a)^2 + \eta^2 + z^2.$$

The integrals in (A-4) have been evaluated analytically in Section 3:

$$\hat{I}_0 = \arctan \frac{zr}{\eta h - z^2 a} - \arctan \frac{z}{\eta}, \tag{A-5}$$

$$\hat{I}_1 = z \ln (r + h + \eta a) - z(a/b) \ln f \tag{A-6}$$

and

$$\hat{I}_2 = z\left(\eta - \frac{a}{b^2} r - \frac{h}{b^3} \ln f\right) - z^2 \hat{I}_0 \tag{A-7}$$

where, as (23), $f = r + \eta b + ha/b$.

To find u_l, we differentiate (A-3) with respect to x under the integral sign. Since x only enters (A-4) through h as in (15), it follows that the equivalent operator to $\partial/\partial x$ in (A-4) is $(-\partial/\partial h)$. So the streamwash is given by (A-3) with $\hat{I}_x$ in place of $\hat{I}$, where

$$\hat{I}_x = \partial\hat{I}/\partial x = -\partial\hat{I}/\partial h = (g_0 - g_2 z^2) \frac{z(ha + \eta b^2)}{r(h^2 + z^2 b^2)} + \left(g_1 z \frac{a}{b} + g_2 z \frac{h}{b^3}\right) \frac{h + \eta a + ra/b}{rf}$$
$$- g_1 \frac{z}{r} + g_2 \frac{z(h + \eta a)a}{rb^2} + g_2 \frac{z}{b^3} \ln f \tag{A-8}$$

We can verify that (A-8) gives the correct answer in the limit $z \to 0+$. Outside a small neighbourhood of the control point (x, y), $\hat{I}_x = 0$ for $z = 0$. At the control point, $\partial \hat{I}_0/\partial h$ is singular; also, by (15), $h = 0$. On the control strip $\eta_- < 0$, $\eta_+ > 0$, h is just the distance downstream of the control point, and we take our small neighbourhood to be $-\varepsilon \leqslant h \leqslant \varepsilon$. Changing the chordwise variable to h, and replacing $(g_0/c \sin \phi)$ by its value $l(x, y)$ at $h = 0$, we have the integral in (A-3) rewritten for u_l

$$\frac{1}{2}\int_0^{\pi} d\phi[\hat{I}_x(\eta)]_{\eta_-}^{\eta_+} = \frac{1}{2}\int_{-\varepsilon}^{\varepsilon}\left(\frac{2}{c \sin \phi}\,dh\right)\left[-g_0\frac{\partial \hat{I}_0}{\partial h}\right]_{\eta_-}^{\eta_+}$$

$$= -l(x, y)\left[\left[\arctan\frac{zr}{\eta h - z^2 a} - \arctan\frac{z}{\eta}\right]_{\eta_-}^{\eta_+}\right]_{-\varepsilon}^{\varepsilon} + O(z).$$

Now keep ε fixed and let $z \to 0$. The second arctangent is independent of h and does not contribute. Since $r > 0$, the first one contributes

$$-l(x, y)\left[\left[\arctan\frac{0+}{(\operatorname{sgn} h)(\operatorname{sgn} \eta)}\right]_{\eta_-}^{\eta_+}\right]_{-\varepsilon}^{\varepsilon} = -l(x, y)\{(0 - \pi) - (\pi - 0)\} = 2\pi l(x, y)$$

so (A-3) gives

$$u_l(x, y, 0) = \tfrac{1}{4}l(x, y).$$

To find the sidewash v_l, we differentiate (A-3) with respect to y under the integral sign. Now, from (15) and the definition $Y - y = \eta$, we have

$$\frac{\partial}{\partial y} = a\frac{\partial}{\partial h} - \frac{\partial}{\partial \eta} \tag{A-9}$$

as the equivalent operator to use on $\hat{I}_0$, $\hat{I}_1$, $\hat{I}_2$ in (A-4). The coefficients g_n also depend on y, for (11) is an expansion about $Y = y$; to see this, write it first as an expansion about $Y = 0$:

$$L = L_0 + YL_1 + Y^2L_2$$

in which the L_n depend only on the initial data for L, and then substitute for Y:

$$L = L_0 + (y + \eta)L_1 + (y + \eta)^2L_2$$

from which

$$g_0 = L_0 + yL_1 + y^2L_2,$$
$$g_1 = L_1 + 2yL_2$$

and

$$g_2 = L_2$$

and so

$$\frac{dg_0}{dy} = g_1; \qquad \frac{dg_1}{dy} = 2g_2; \qquad \frac{dg_2}{dy} = 0. \tag{A-10}$$

Applying (A-9) to the $\hat{I}_n$, and (A-10) to the g_n, v_l is given by (A-3) with $\hat{I}_y$ in place of $\hat{I}$, where

$$\hat{I}_y = \sum_{n=0}^{2}\left[g_n\left(a\frac{\partial \hat{I}_n}{\partial h} - \frac{\partial \hat{I}_n}{\partial \eta}\right) + \frac{dg_n}{dy}\cdot \hat{I}_n\right].$$

Making use of (A-4) and (A-8), this gives

$$\hat{I}_y = -a\hat{I}_x - z\frac{g_0 + \eta g_1 + \eta^2 g_2}{\eta^2 + z^2}\left(1 - \frac{h + \eta a}{r}\right) + g_1\hat{I}_0 + 2g_2\hat{I}_1 \tag{A-11}$$

with $\hat{I}_0, \hat{I}_1$ from (A-5), (A-6).

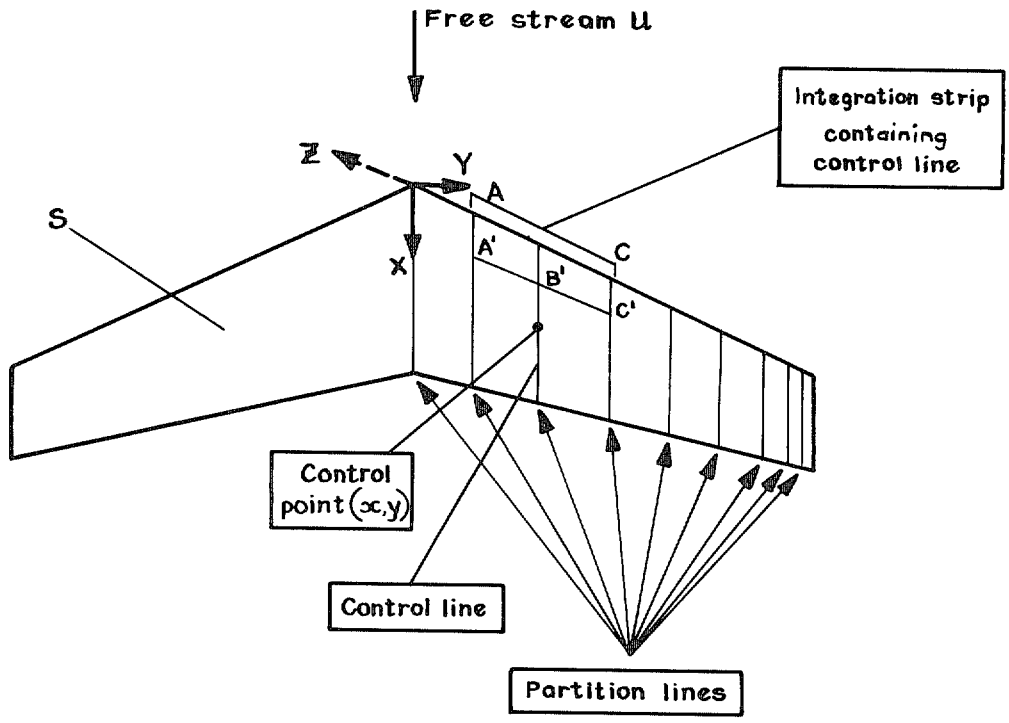

FIG. 1. Spanwise partitioning of wing.

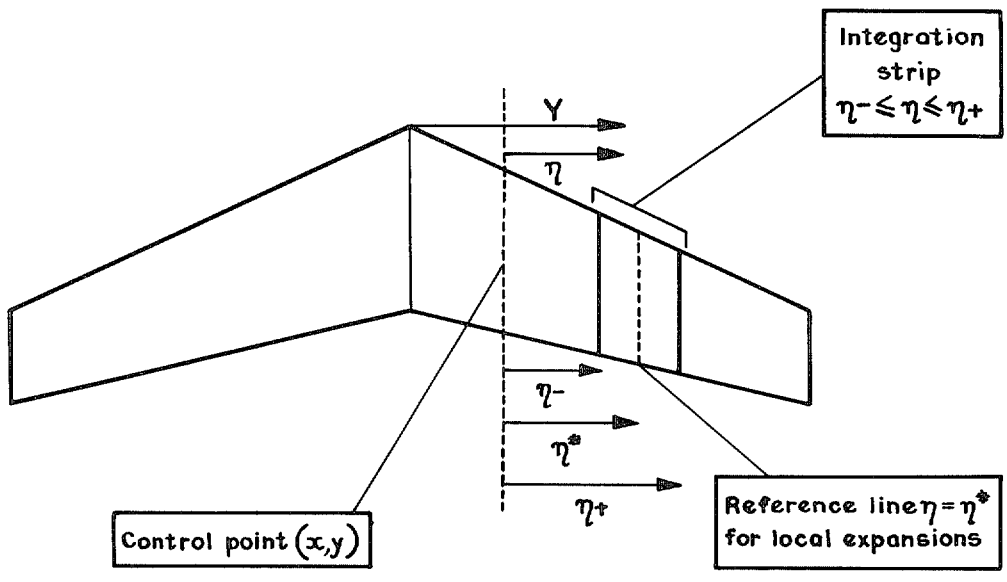

FIG. 2. Spanwise coordinate system relative to the control line.

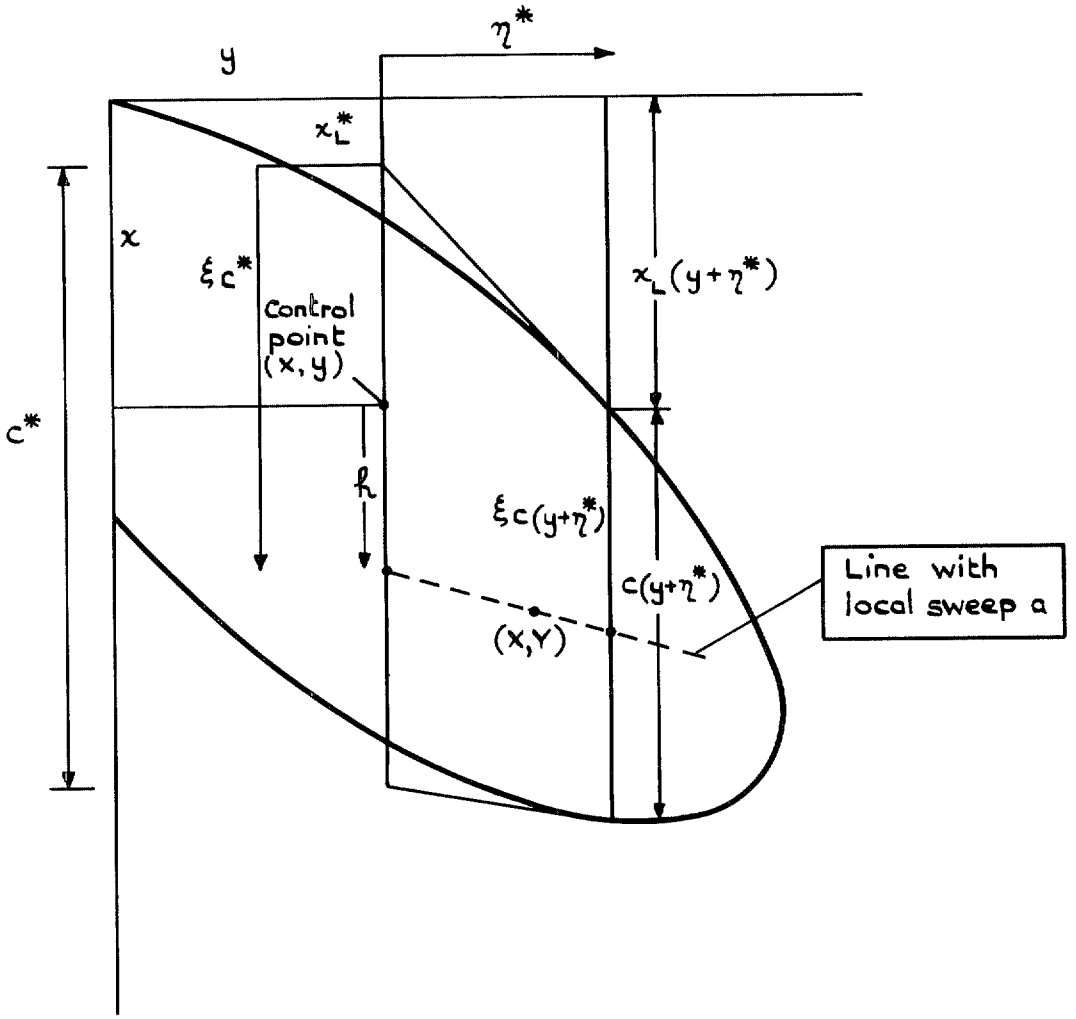

FIG. 3. Physical meaning of x_L^*, c^* and h.

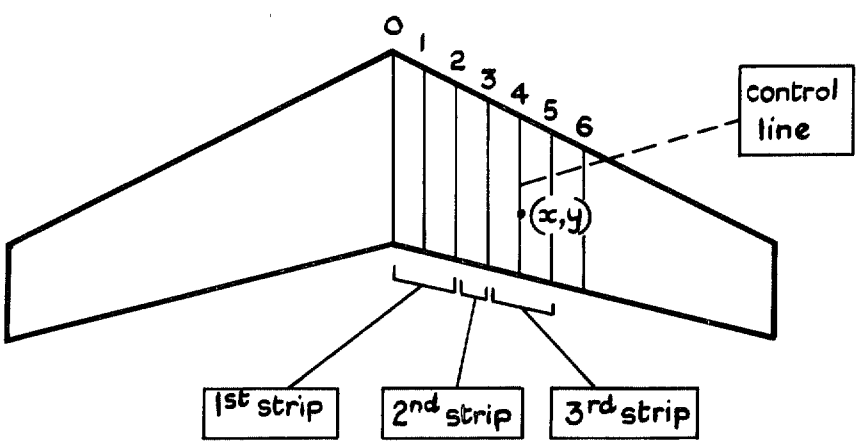

FIG. 4. Choice of integration strips relative to centre line and control line.

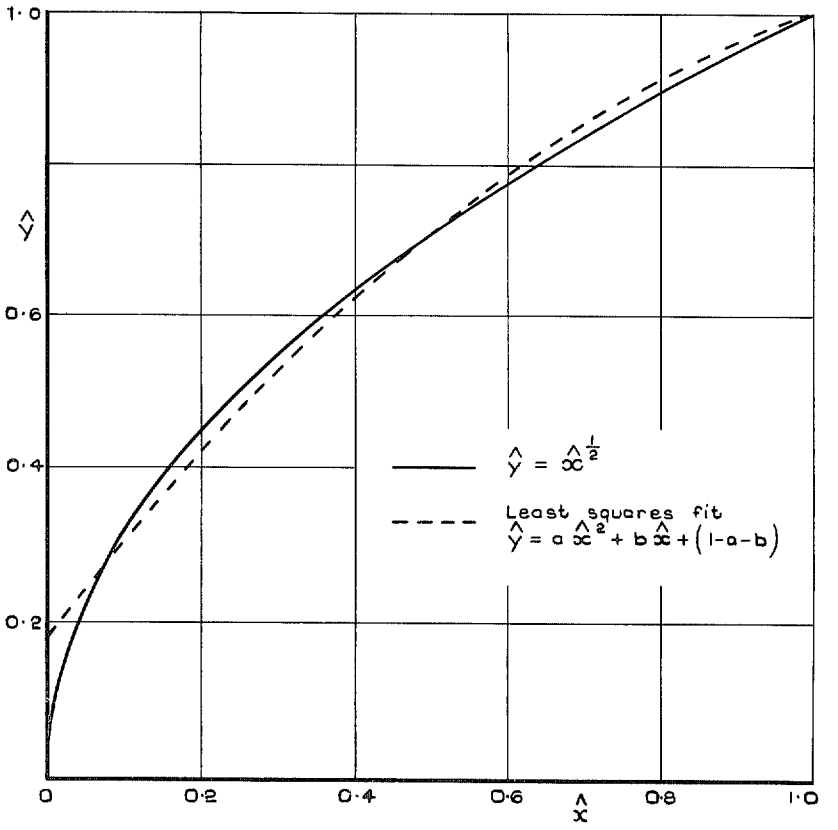

FIG. 5. Parabolic least squares approximation to wing tip loading.

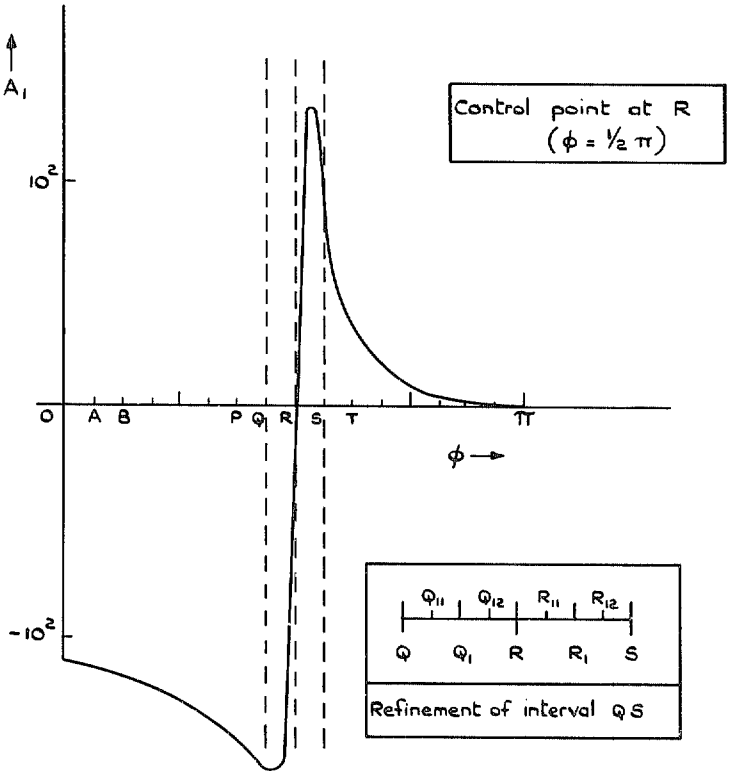

FIG. 6. Typical chordwise variation of A_1 on control strip.

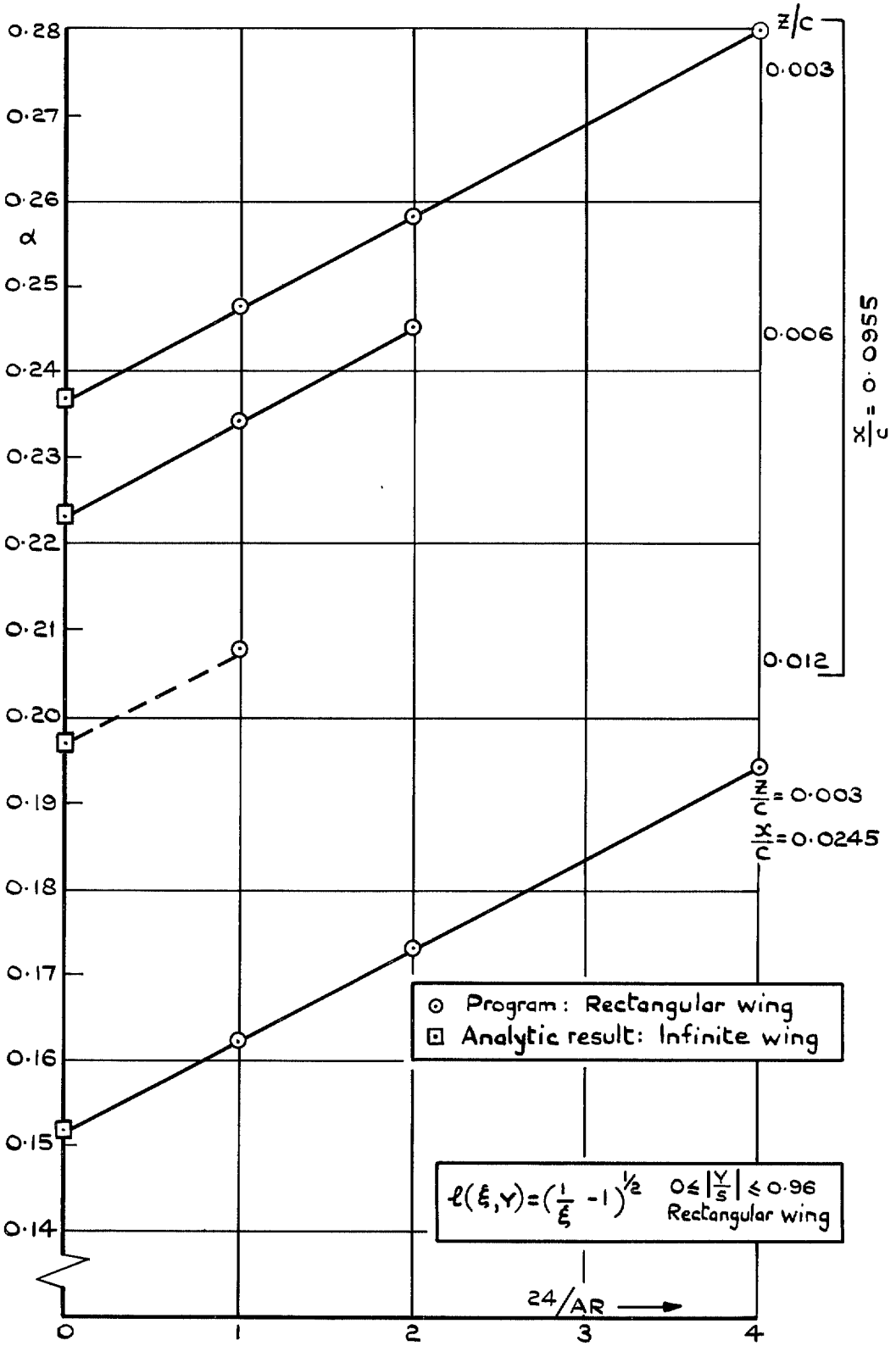

FIG. 7. Downwash as function of aspect ratio. Rectangular wing.

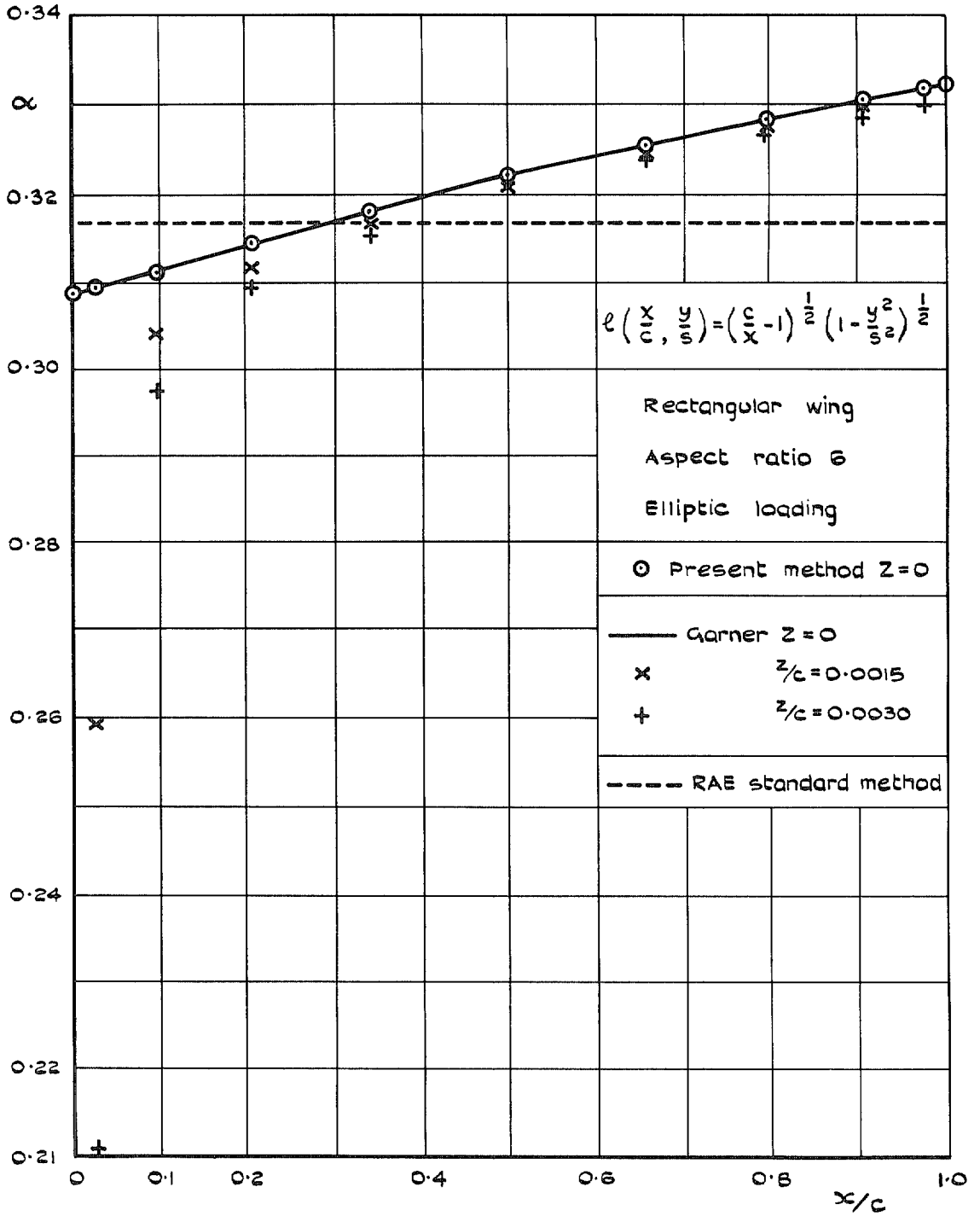

FIG. 8. Downwash on centre line. Check with Garner's theory.

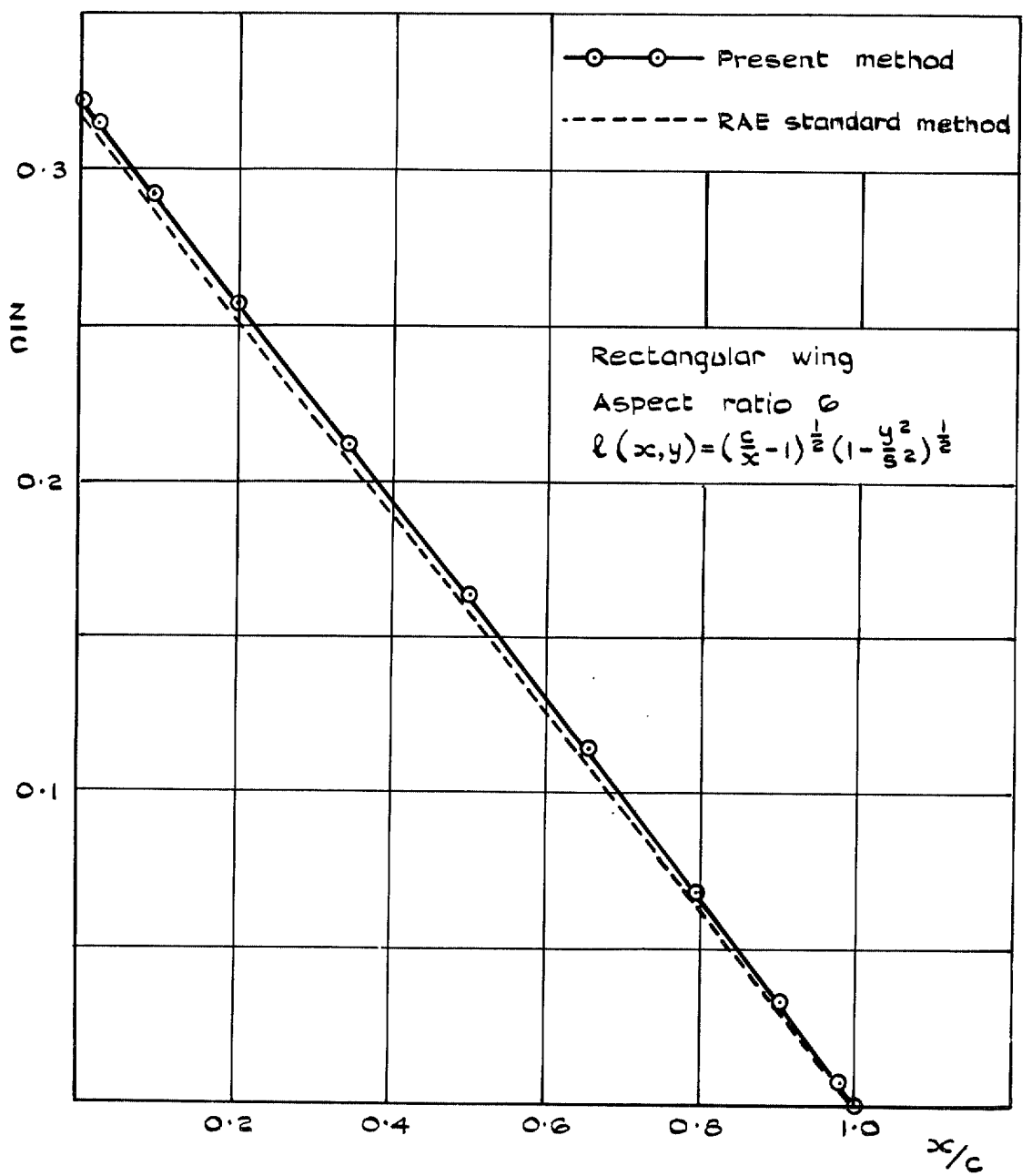

FIG. 9. Centre line ordinates from downwash calculations.

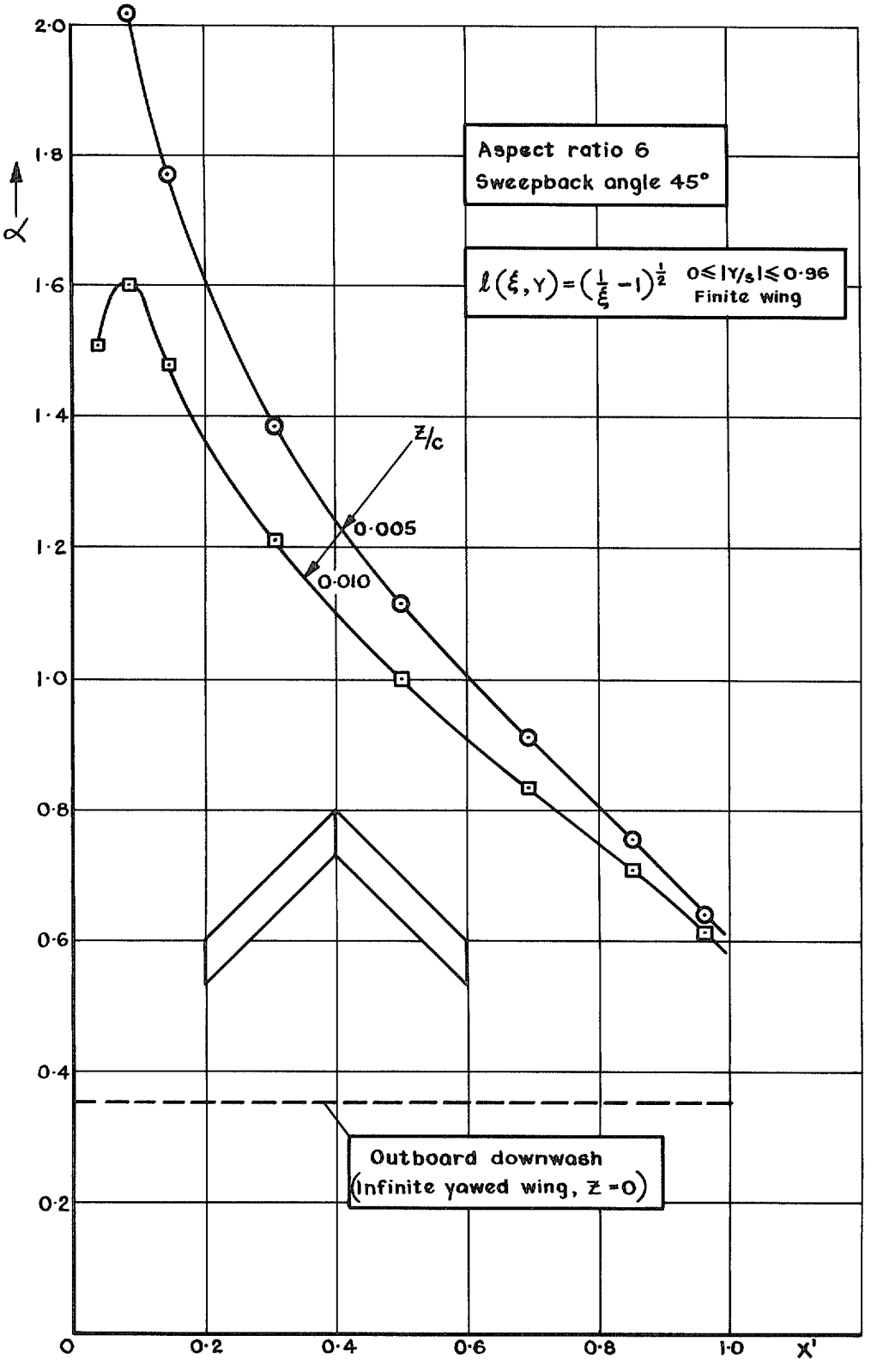

FIG. 10. Downwash on centre section of constant chord wing.

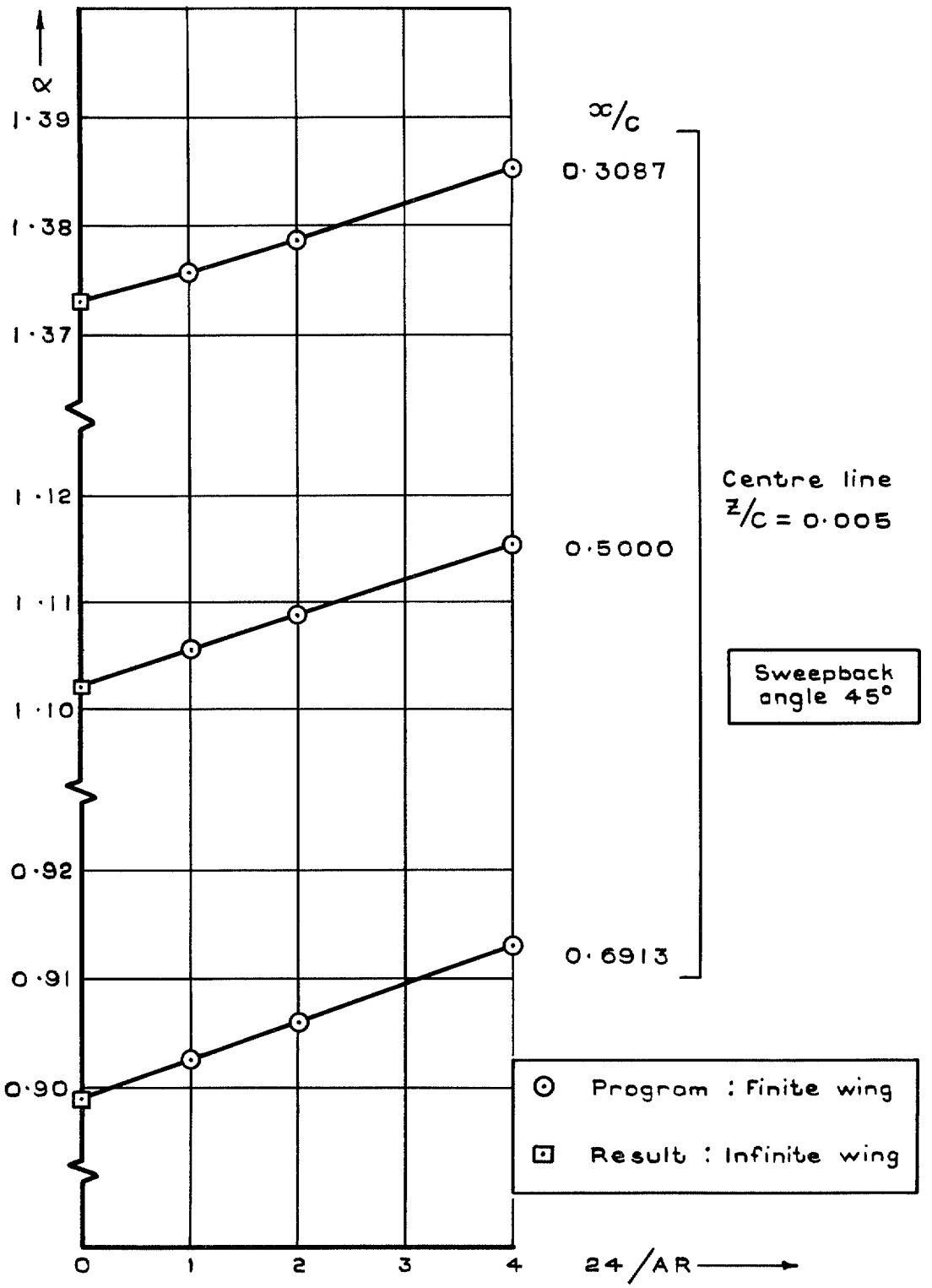

FIG. 11. Downwash as function of aspect ratio. Constant chord wing.

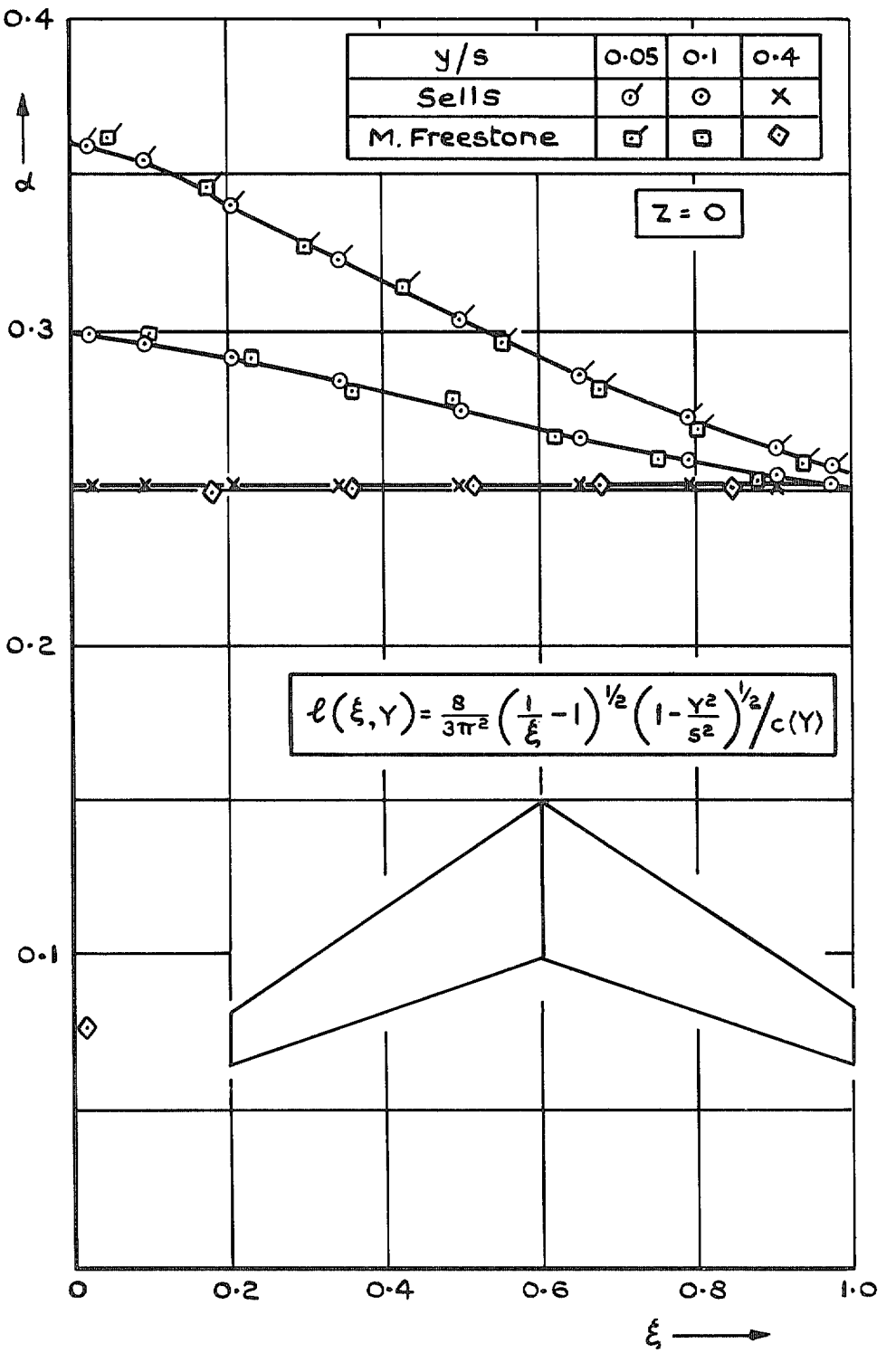

FIG. 12. Chordwise distribution of downwash on R.A.E. wing 'A'. Comparison with Freestone's program.

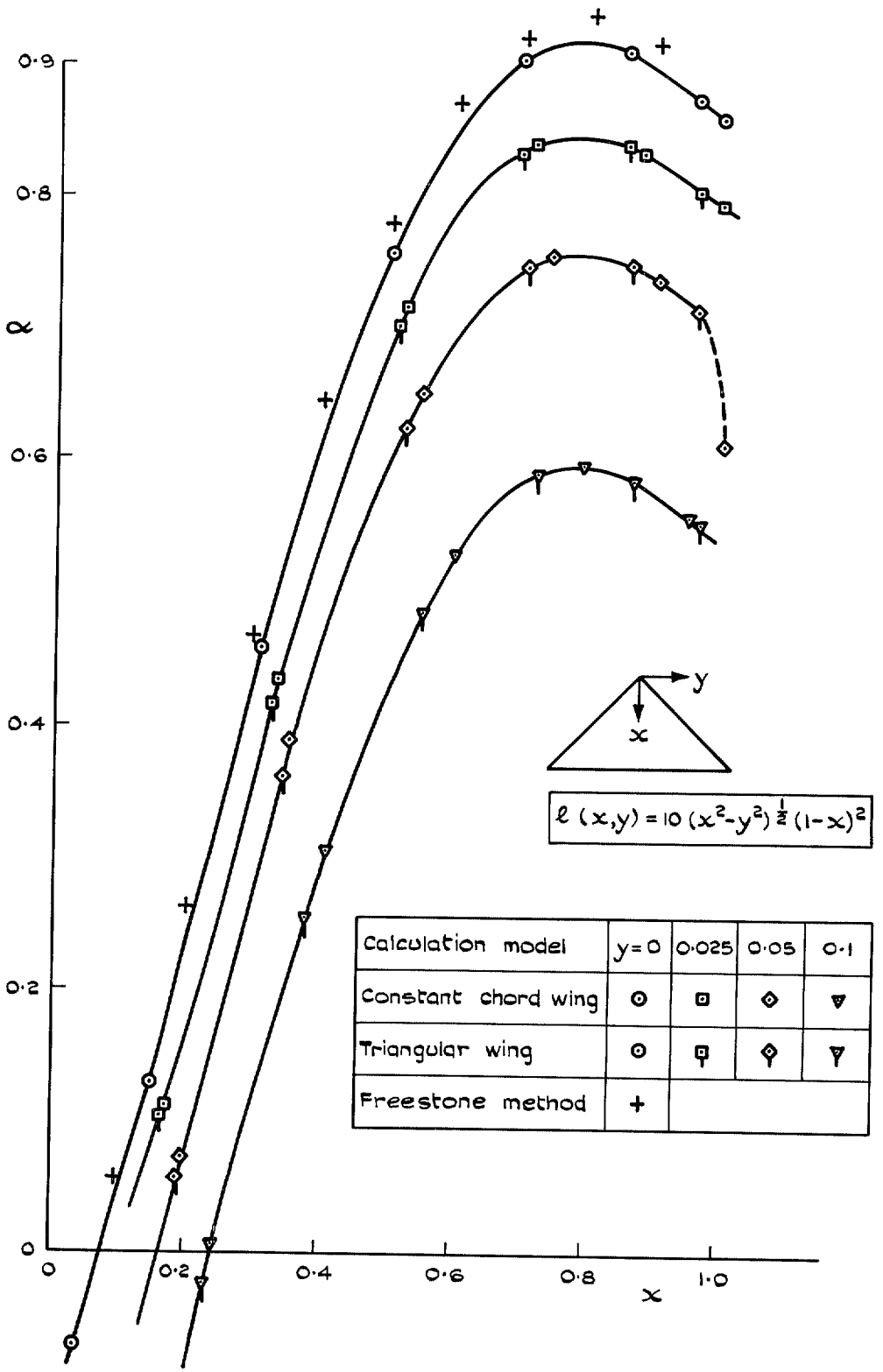

FIG. 13. Downwash near centre line of delta wing with rounded isobars.

Printed in England for Her Majesty's Stationery Office by J. W. Arrowsmith Ltd., Bristol BS3 2NT
Dd. 505715 K5 6/73

HER MAJESTY'S STATIONERY OFFICE

Government Bookshops

49 High Holborn, London WC1V 6HB
13a Castle Street, Edinburgh EH2 3AR
109 St Mary Street, Cardiff CF1 1JW
Brazennose Street, Manchester M60 8AS
50 Fairfax Street, Bristol BS1 3DE
258 Broad Street, Birmingham B1 2HE
80 Chichester Street, Belfast BT1 4JY

Government publications are also available through booksellers

SBN 11 470525 9